MALACOLOGIA, 2010, 52(1): 115–153

ANATOMY OF THE TIPHOBIINI FROM LAKE TANGANYIKA (CERITHIOIDEA, PALUDOMIDAE)

Ellen E. Strong[1]* & Matthias Glaubrecht[2]

ABSTRACT

The anatomy of five poorly known endemic species of paludomids – *Bathanalia straeleni*, *Chytra kirkii*, *Limnotrochus thomsoni*, *Mysorelloides multisulcata*, *Paramelania iridescens* – from Lake Tanganyika is described. This assemblage, currently united in the Tiphobiini, is loosely characterized by a more or less trochiform shell shape and a mostly oviparous life mode. However, only scant information on the anatomy is available in the literature. Despite significant conchological variability, anatomical investigations reveal overriding similarity in features of the alimentary system (radula, midgut), kidney, and reproductive anatomy. *Bathanalia* and *Mysorelloides* are found to share features of the ovipositor, esophagus and spermatophore bursa; *Chytra* and *Limnotrochus* share features of the salivary glands and spermatophore bursa. *Paramelania* remains a clear outlier in shell morphology, but shares several likely plesiomorphic features of the operculum, midgut and nervous system with *Tiphobia*. Unlike other morphologically distinct clades of Lake Tanganyika paludomids, no unique anatomical character was found that unambiguously unites the Tiphobiini.

Key words: freshwater, morphology, shell, alimentary system, reno-pericardial system, nervous system, reproductive system.

INTRODUCTION

The spectacular endemic species assemblage of phenotypically diverse paludomid gastropods in Lake Tanganyika comprises approximately 70 species (Michel, 2004). As discussed elsewhere (Glaubrecht, 1996, 1999, 2008; Strong & Glaubrecht, 2002), the divergent conchological features of Lake Tanganyika gastropods, combined with inadequate knowledge of their internal anatomy, have left their mark in a chaotic and confusing classification. What little anatomy was known was too unremarkable to reveal their true affinities and was easily misconstrued.

The first series of anatomical papers was published around the turn of the century (Moore, 1898, 1899a, b, 1903; Digby, 1902), and remained all that was known of these forms for roughly 50 years until the Belgian hydrobiological mission to the lake in 1946–1947. This period of renewed interest resulted in the publication by Leloup (1953) that documented the operculum and radula of numerous lake gastropods, many for the first time, and several anatomical studies (Mandahl-Barth, 1954; Bouillon, 1955). This was followed again by a long hiatus until the modern age of investigation, which has yielded a series of anatomical and molecular studies (West & Michel, 2000; Michel, 2004; Wilson et al., 2004; Strong & Glaubrecht, 2002, 2003, 2007, 2008; Glaubrecht & Strong, 2004, 2007).

Despite this long history of inquiry, many of these endemic gastropods remain poorly known, some more than others, including a loose-knit group of oviparous and ovoviviparous species with more or less trochiform shells currently classified with *Tiphobia horei* Smith, 1880, in the Tiphobiini Bourguignat, 1886 (Bouchet & Rocroi, 2005): *Bathanalia straeleni* Leloup, 1953; *Chytra kirkii* (Smith, 1880); *Limnotrochus thomsoni* Smith, 1880; *Mysorelloides multisulcata* (Bourguignat, 1888); and *Paramelania iridescens* (Moore, 1898). With the exception of *Tiphobia horei*, which was recently redescribed (Strong & Glaubrecht, 2007), virtually nothing is known about these species. Available anatomical descriptions of *Chytra kirkii*, *Limnotrochus*

---

[1] Smithsonian Institution, National Museum of Natural History, P.O. Box 37012, MRC 163, Washington D.C. 20013-7012, U.S.A.

[2] Museum für Naturkunde, Leibniz Institute for Research in Evolution and Biodiversity, Invalidenstrasse 43, D-10115 Berlin, Germany

*Corresponding author: stronge@si.edu

thomsoni, and *Paramelania iridescens* were published over a century ago and are woefully incomplete (Digby, 1902; Moore, 1898, 1899b, 1903). Only scant information on the radula and operculum are known for *Bathanalia straeleni* and *Mysorelloides multisulcata* (Leloup, 1953). While the congener *Bathanalia howesi* Moore, 1898, has been included in molecular analyses (West & Michel, 2000; Michel, 2004), *B. straeleni* has not, and no sequences are available for *Mysorelloides*, rendering any anatomical information all the more critical for understanding its affinities.

Although not always reflected in their classification, suggested affinities of tiphobiines have been rooted in their conchological attributes. *Limnotrochus* and *Chytra* possess shells that closely approximate a typical trochoid construction (Smith, 1881; Ancey, 1882; Yonge, 1938). *Bathanalia* and *Mysorelloides*, while not as solid and lacking the nodulose ornament, possess similarly umbilicate shells. The ovoviviparous *T. horei* possesses a shell that is umbilicate in juveniles, with a prominent keel similar to *Limnotrochus*, *Chytra* and *Bathanalia*, and produces spines along the keel like *Bathanalia howesi*. *Paramelania*, with its rather high, conical spire, thickened holostomous aperture, rounded whorl profile, and lacking an umbilicus, is the least well accommodated among this assemblage.

Consequently, *Chytra* and *Limnotrochus* have been cited as closely related, *Bathanalia* with *Tiphobia*, and *Paramelania* acknowledged to resemble *Lavigeria*, but classified in an isolated position based on shell, operculum and radula characters (i.e., "*Limnotrochus* group", "*Tiphobia* group", and "*Paramelania* group", respectively; Pilsbry & Bequaert, 1927). Thiele's (1929–1935) classification marked a significant departure from previous views, uniting the tiphobiine taxa with *Bridouxia*, *Reymondia*, *Spekia*, *Stanleya*, *Stormsia* and *Tanganyicia* in a Tribe Paramelaniini, but he failed to recognize nomenclatural priority of the family-group name Tiphobiidae Bourguignat, 1886, for this assemblage. Recently, Bandel (1998) proposed a classification that reinstated the isolated positions of *Paramelania* and *Tiphobia* in separate subfamilies citing features of the shell, operculum, radula and reproductive modes (oviparous vs. ovoviviparous) and tentatively suggested that *Bathanalia*, *Chytra*, *Limnotrochus* and *Mysorelloides* may be united, but that current knowledge did not allow assigning them to one of the recognized subfamilies. In contrast, Glaubrecht (2008) largely followed Thiele's concept of Paramelaniini, united by the presence of a concentric operculum with a spiral nucleus, but subgroups within this assemblage were distinguished by radular morphologies and similar radulae were assumed to have arisen in parallel in other subfamilies.

Molecular analyses have generally supported tiphobiine taxa as closely related, although taxon sampling of different studies has not been comparable, and no molecular sequences are available for *Mysorelloides*. In an analysis of partial mitochondrial COI sequences, West & Michel (2000) found support for a clade with available tiphobiine taxa – *Bathanalia*, *Chytra*, *Limnotrochus*, *Paramelania*, *Tiphobia* – but which also included *Anceya* and sometimes *Lavigeria*. However, anatomical studies (Strong & Glaubrecht, 2007, 2008) demonstrate the distinctiveness of the latter two and that their affinities likely lie elsewhere. In an analysis of partial mitochondrial 16S and COI sequences with a larger subset of lake taxa, Wilson et al. (2004) recovered a clade uniting *Limnotrochus*, *Paramelania* and *Tiphobia*, but *Bathanalia*, *Chytra* and *Mysorelloides* were not sequenced. Michel's (2004) results, based again on partial COI sequences, supported a monophyletic Tiphobiini (excluding *Mysorelloides*). This molecular evidence, in the context of available morphological data including that presented herein, formed the basis for the classification in Bouchet & Rocroi, which acknowledged that the Tiphobiini may be paraphyletic (Strong, pers. comm. in Bouchet & Rocroi, 2005: 275). The goal of this contribution is to explore this anatomical data and to assess the relationships suggested by molecular data in an anatomical context.

MATERIAL AND METHODS

Anatomical Descriptions

The scarcity of well-preserved alcohol material in museum collections has been an impediment to anatomical investigations of Lake Tanganyika gastropods. For some species, alcohol preserved material is rare (*Bathanalia straeleni*, *Mysorelloides multisulcata*, *Chytra kirkii*), for others the alcohol material is of poor quality, typically reflecting the fact that specimens were placed in preservative without cracking the shell. For small species, specimens placed whole into alcohol are often salvageable as the volume of tissue is small. But for large species, if the shell is not broken they can be too poorly preserved for even basic anatomical observations. In the present investigation, only a single female of *B. straeleni* (IRSNB), two females of *M. multisulcata* (IRSNB), and a single male and female of *C. kirkii* (IRSNB, USNM) were available for study from museum collections. Study of *Limnotrochus* and *Paramelania* was based on recent collections by Klaus Bandel (Hamburg) and MG in 1995, Anthony Wilson (Zurich) in 1999 and 2000, and by Heinz H. Büscher (Basel) in 2003, but only one of these specimens was cracked prior to fixation; two females and one male were examined for *Limnotrochus thomsoni* and for *Paramelania iridescens* four specimens were dissected, but only one had an adequately preserved midgut and only two had adequately preserved gonoducts to allow accurate descriptions. Specimens were examined using Leica MZ 9.5 or MZ 12.5 binocular microscopes with *camera lucida*; visualization of structural details was enhanced with aqueous toluidine blue.

Formula for radular tooth descriptions is as follows: (1) rachidian: number of denticles on left side/median cusp/number of denticles on right side, (2) lateral teeth: inner denticles/pronounced cusp/outer denticles, (3) marginal teeth: number of denticles on inner marginal tooth/number of denticles on outer marginal tooth.

Midgut investigations were completed by making an incision around the exposed periphery of the midgut chamber along the right, anterior and posterior margins and deflecting the roof to the left.

Museum Codes

AMS	Australian Museum, Sydney, Australia
CM	Carnegie Museum, Pittsburg, Pennsylvania, U.S.A.
BMNH	The Natural History Museum, London, U.K.
DBL	Danish Bilharziasis Laboratory, Charlottenlund, Denmark
IRSNB	Institut Royal des Sciences Naturelles de Belgique, Brussels, Belgium
MNHN	Muséum National d'Histoire Naturelle, Paris, France
MRAC	Musée Royal de l'Afrique Central, Tervuren, Belgium
NHMB	Naturhistorisches Museum, Basel, Switzerland
ZMB	Museum für Naturkunde, Leibniz Institute for Research in Evolution and Biodiversity, Berlin (formerly Zoologisches Museum Berlin), Germany

RESULTS

Bathanalia straeleni
Leloup, 1953

Material Examined: Democratic Republic of Congo: off Cape Bwana n'Denge, 1,000 m offshore along the coast, trawling starting 3 mi [4.83 km] NW of Lugumba until in front of Lukuga River, 20–80 m (IRSNB no. 50) (1 "paratype" dissected = syntype, as no (holo) type was designated by Leloup, 1953); Katibili Bay, 500 m from the river, 65–70 m (IRSNB no. 133) (58 spms); Bracone Bay, Kavala Island, 12 m (IRSNB no. 138) (16 spms). Tanzania: Utinta Bay, 45–65 m (IRSNB no. 127) (1 spm); bay to the south of the Malagarasi River (IRSNB no. 143) (2 spms).

Shell: Adult shell comprising up to seven whorls (Fig. 1). Apical cap of embryonic shell with irregularly, finely textured surface, rapidly giving way to numerous fine spiral threads (Figs. 2, 3). Gradual transition to teleoconch marked by development of regular, thick axial threads, peripheral keel at shoulder and basal spiral cord sometimes visible just above suture. Early teleoconch whorls angular. Axial elements forming nodes at intersection with keel. Basal cord joined on later teleoconch whorls by variable number of smoothly undulating spiral cords on lower half of whorl. Keel and nodular ornament gradually diminishing, producing flatly rounded later teleoconch whorls with fine, sigmoidal growth lines and basal spiral cords. Aperture thickened, with weakly developed anterior and posterior siphons. Umbilicus narrow. Shell microstructure (Fig. 4) comprising four layers from external to internal: (1) irregular, simple prismatic structure, (2) simple radial crossed lamellar structure, (3) simple comarginal crossed lamellar structure, (4) irregular, simple prismatic structure.

External Anatomy: Operculum (Fig. 7) thin, transparent, light amber brown in color. Operculum spiral, comprising approximately six whorls, increasing evenly in size.

Foot narrowly ovate, with narrow propodium bearing shallow pedal gland along anterior margin (Fig. 6: ap). Columellar muscle extending to base of mantle cavity. In females, ovipositor (Fig. 6: ovp) present on right side of foot, below eye, just behind foot sole margin. Aperture of ovipositor forming simple, oblique slit bounded by inflated folds; lumen

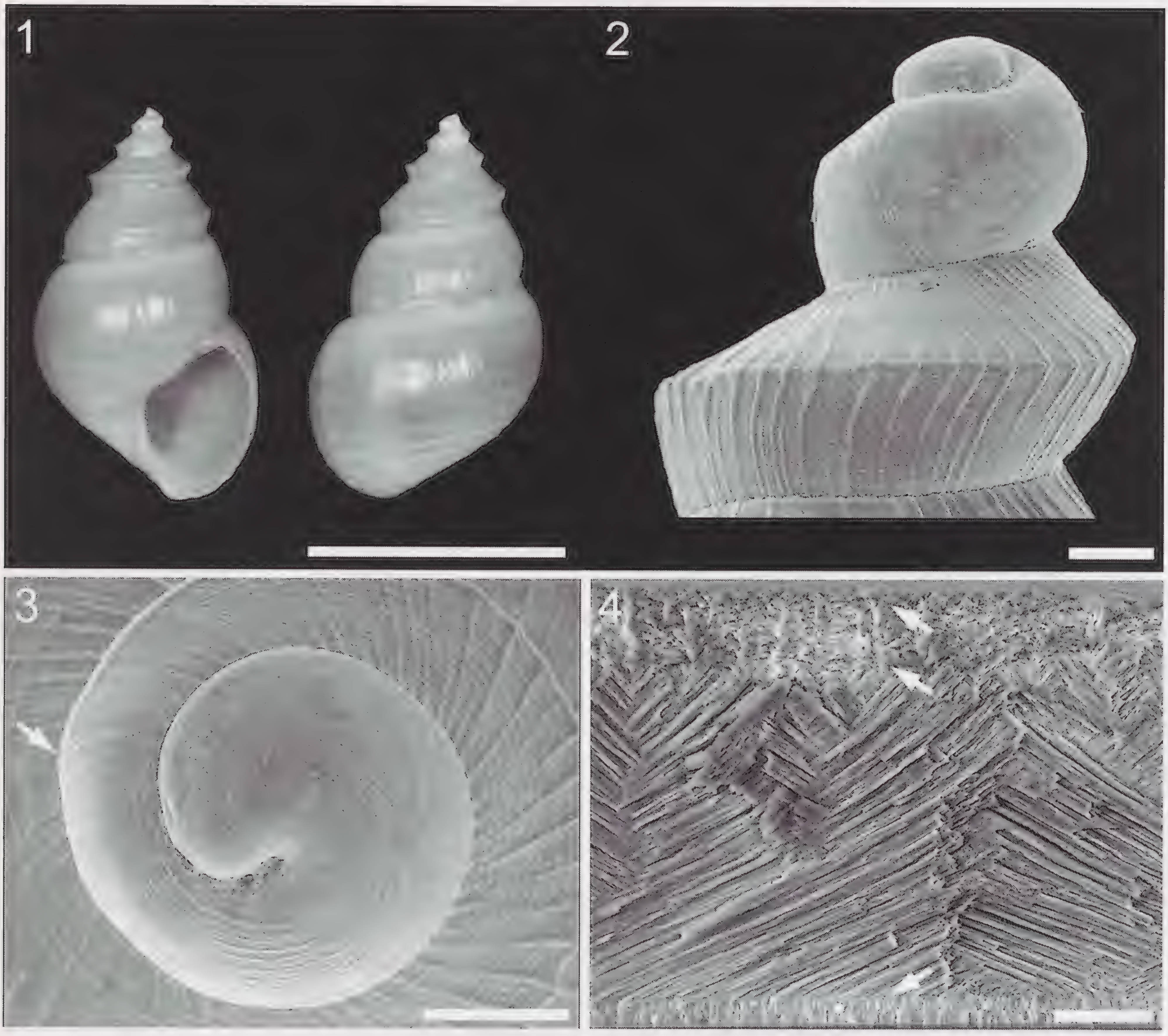

FIGS. 1–4. Shell morphology of *Bathanalia straeleni* (IRSNB no. 133, except when noted). FIG. 1: Adult shell. Scale bar = 5 mm; FIG. 2: Embryonic shell. Scale bar = 100 µm; FIG. 3: Embryonic shell, apical view. Arrow indicates approximate transition to teleoconch. Scale bar = 100 µm; FIG. 4: Shell microstructure (IRSNB no. 50). Cross section through shell parallel to aperture; outside of shell is uppermost. Order of layers from external to internal: (a) irregular, simple prismatic structure, (b) simple radial crossed lamellar structure, (c) simple comarginal crossed lamellar structure, (d) irregular, simple prismatic structure. Arrows indicate transitions between layers. Scale bar = 20 µm.

u-shaped with prominent fold projecting from floor. Finely grooved tract extending from pore, intersecting foot sole near anterior end of mesopodium. Ciliated egg groove between ovipositor and pallial oviduct lacking.

Retracted cephalic tentacles (Figs. 6, 8: t) smooth, short, thick, slightly longer than snout. Eyes located on small protuberances at base of tentacles. Snout (Fig. 8: sn) squarish, tapering to small mouth opening ventrally at tip.

Mantle cavity short, extending approximately one half whorl. Hypobranchial gland well developed (Figs. 5, 8: hg), thick, with transverse grooves. Inhalant margin of mantle edge (Fig. 8: me) with ~8 small papillae. Ctenidium (Figs. 5, 6, 8: ct) extending from near mantle margin to rear of mantle cavity; leaflets narrowly triangular. Osphradium (Figs. 5, 8: os) smooth, short and thick, roughly one third of ctenidium in length, bordered by distinct ridge at left for most of length, becoming obsolete anteriorly.

Alimentary System: Foregut. Single specimen of radula was teratological and could not be used to make accurate observations on cusp

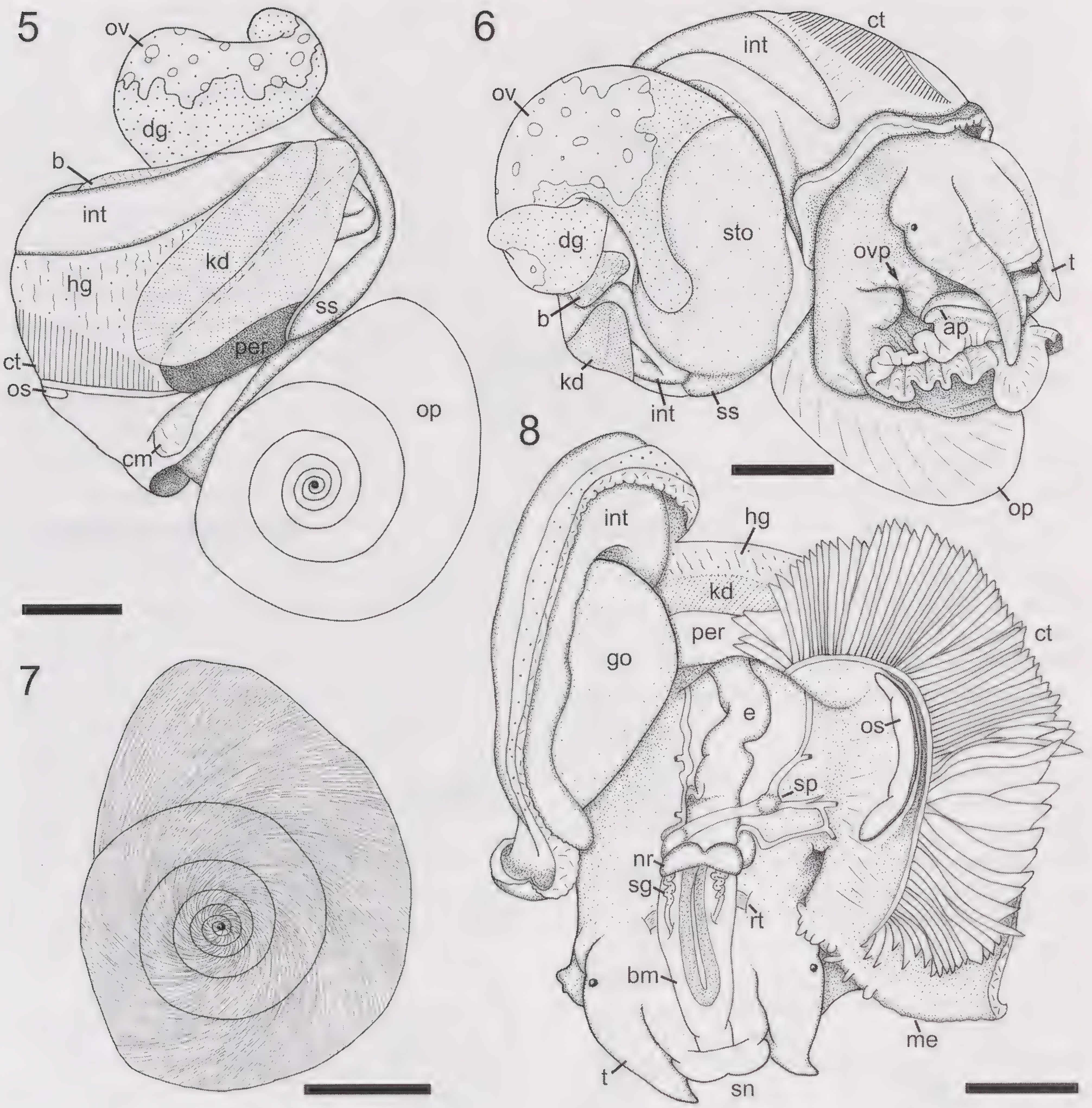

FIGS. 5–8. External anatomy of *Bathanalia straeleni* (IRSNB no. 50). FIG. 5: External view of organs in visceral mass. Dashed line indicates extent of pericardium under main kidney chamber; FIG. 6: External view of organs in visceral mass; right lateral view of female head-foot with ovipositor; FIG. 7: Operculum; FIG. 8: Dorsal view of mantle cavity and organs of cephalic hemocoel seen by transparency. Anterior is below. Abbreviations: ap, anterior pedal gland; b, bladder; bm, buccal mass; cm, columellar muscle; ct, ctenidium; dg, digestive gland; e, esophagus; go, pallial gonoduct; hg, hypobranchial gland; int, intestine; kd, kidney; me, mantle edge; nr, circumesophageal nerve ring; op, operculum; os, osphradium; ov, ovary; ovp, ovipositor; per, pericardium; rt, buccal retractor; sg, salivary gland; sn, snout; sp, supraesophageal ganglion; ss, style sac; sto, stomach; t cephalic tentacle. Scale bars = 1 mm.

morphology. Radula taenioglossate. Rachidian rectangular, roughly two times taller than wide, tapering to v-shaped lower margin. Upper margin slightly concave with cutting edge bearing prominent, central, sharply pointed cusp bounded by pointed denticles on each side. Lateral teeth with extremely long lateral extensions, roughly twice as long as cutting edge. Marginal teeth with long, slender shafts.

Mouth opening ventrally at anterior end of snout. Buccal mass (Fig. 8: bm) narrow,

9

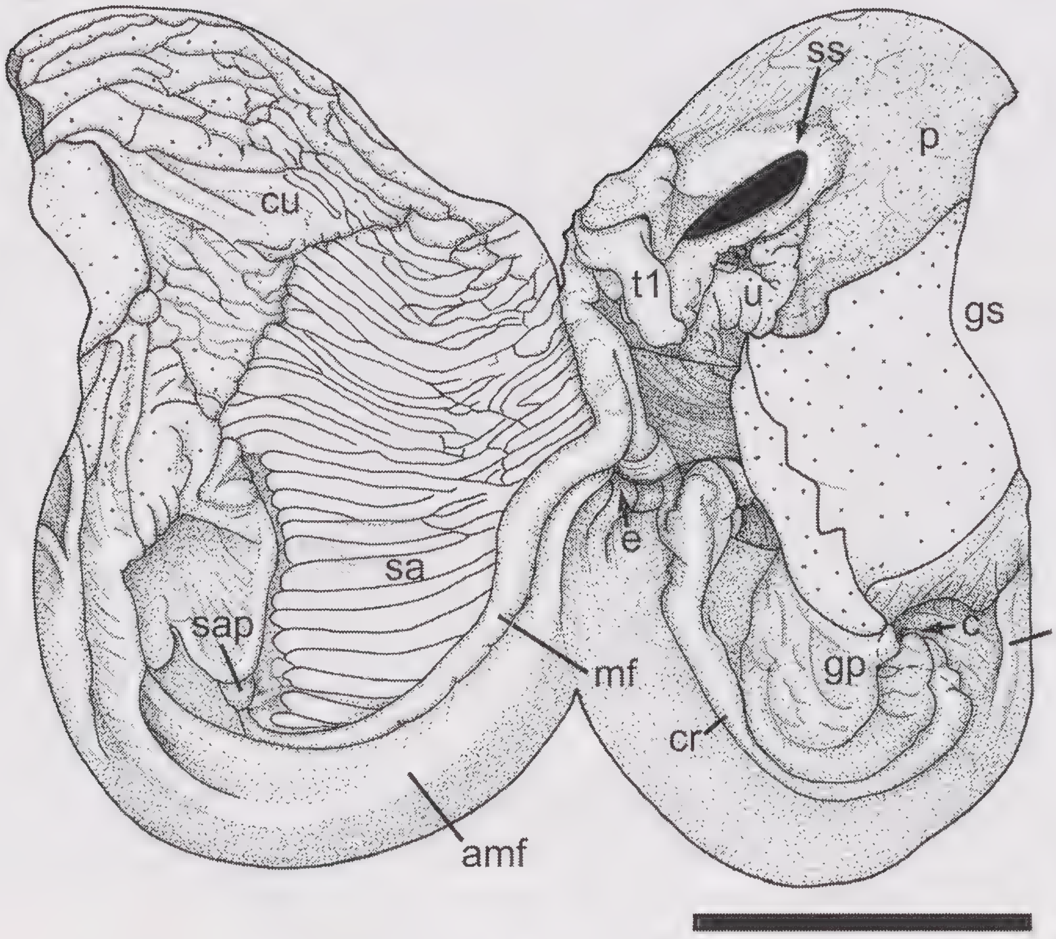

10

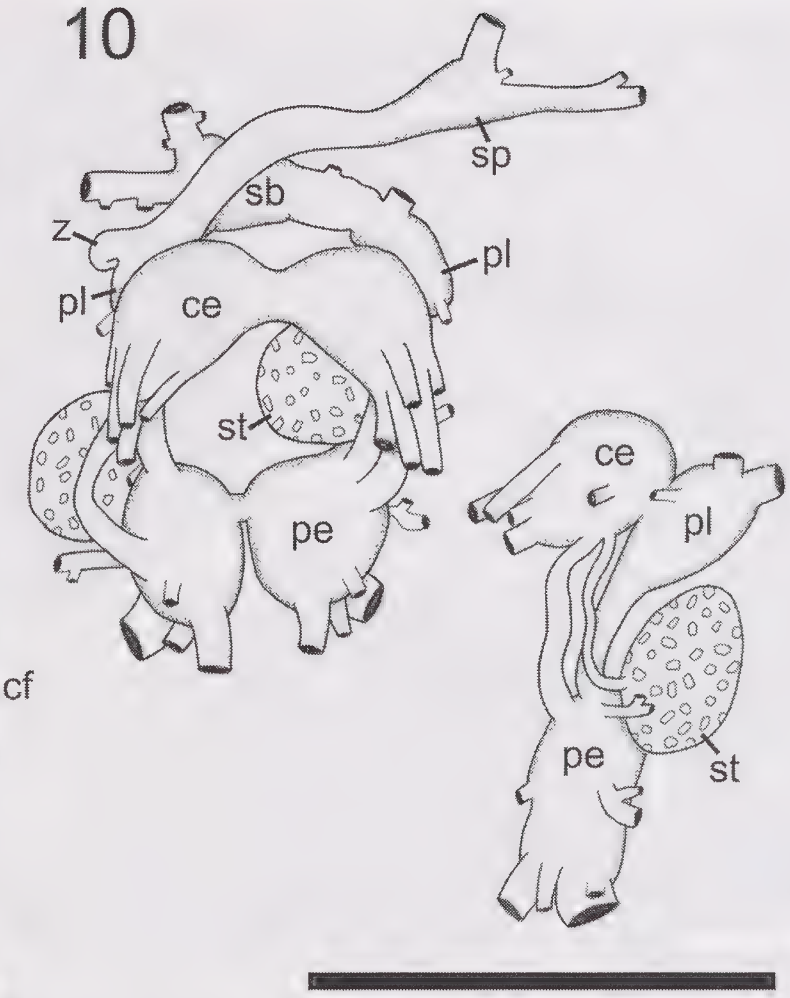

11

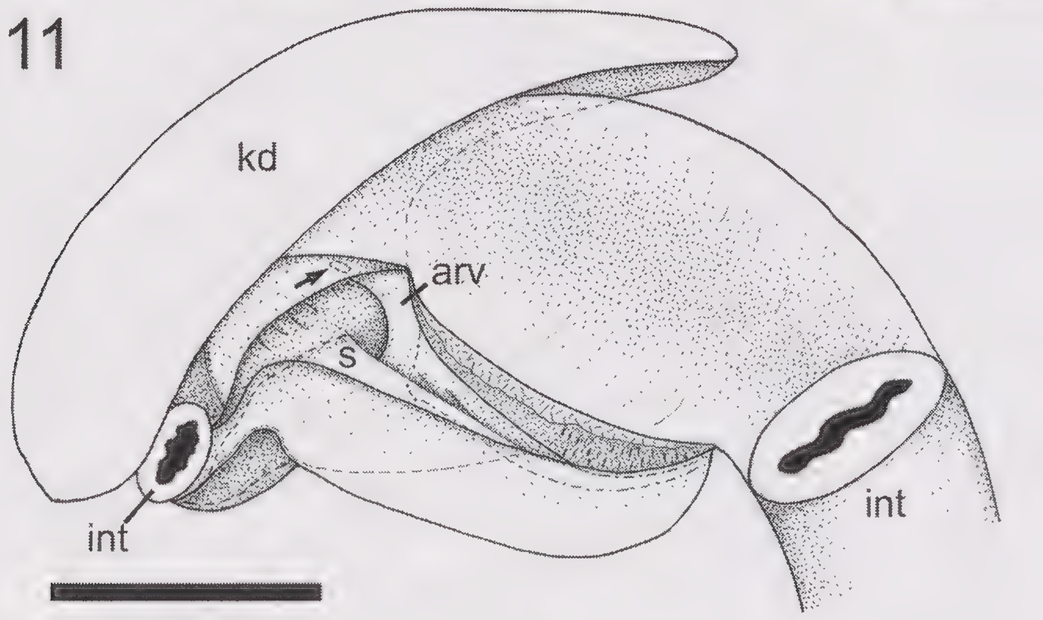

12

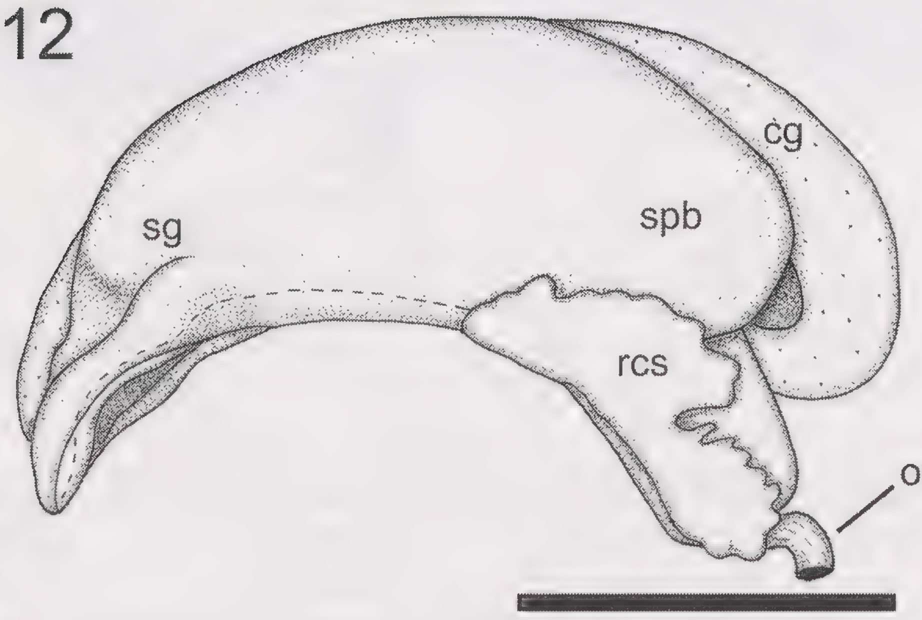

13

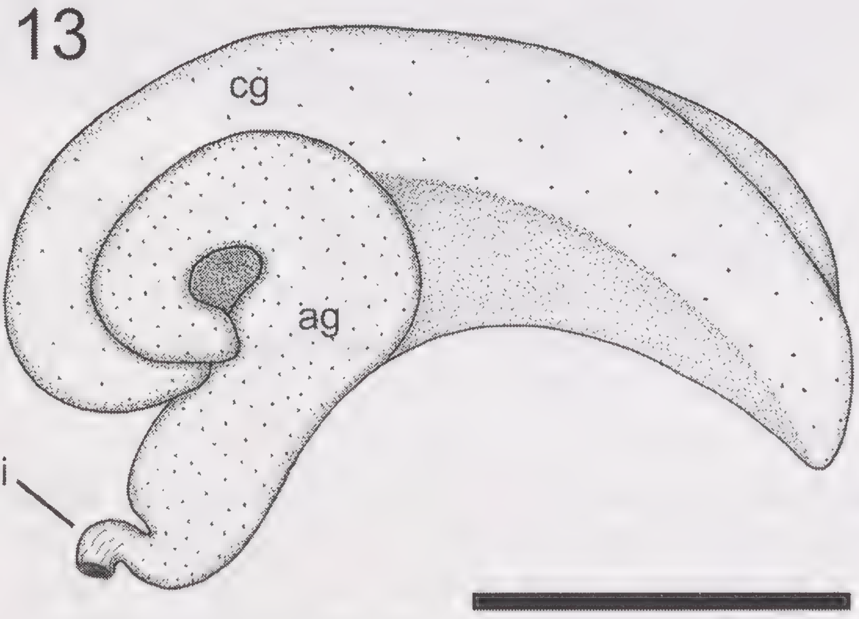

FIGS. 9–13. Internal anatomy of *Bathanalia straeleni* (IRSNB no. 50). FIG. 9: Midgut anatomy. Dorsal view, anterior is uppermost; FIG. 10: Circumesophageal nerve ring. Frontal view (above) and left lateral view (below); FIG. 11: Kidney anatomy. Internal view of bladder. Lateral view, anterior is at right. Roof of bladder (below intestine) cut open to reveal interior; FIG. 12: External, left lateral view of pallial oviduct. Anterior is at left. Single dashed line indicates free ventral edge of inner medial lamina wall, separating spermatophore bursa from gonoductal groove; FIG. 13: External, right lateral view of pallial oviduct. Anterior is at right. Abbreviations: ag, albumen gland; amf, accessory marginal fold; arv, afferent renal vessel; c, caecum; ce, cerebral ganglion; cf, caecal fold; cg, capsule gland; cr, crescentic ridge; cu, cuticularized region in midgut roof; e, esophagus; gp, glandular pad; gs, gastric shield; int, intestine; kd, kidney; mf, marginal fold; ovi, renal oviduct; p, crystalline style pocket; pe, pedal ganglion; pl, pleural ganglion; rcs, seminal receptacle; s, septum; sa, sorting area; sap, sorting area pad; sb, subesophageal ganglion; sg, seminal groove; sp, supraesophageal ganglion; spb, spermatophore bursa; ss, style sac; st, statocyst; t1, major typhlosole; u, u-shaped fold; z, zygoneury. Scale bars = 1 mm.

elongate; small odontophore occupying posterior half of buccal cavity. Narrowly triangular, glandular subradular organ extending along floor of buccal cavity at anterior end of odontophore. Small, paired jaw dorsally flanking mouth at anterior ends of dorsal folds. Shallow, nonglandular buccal pouches extending underneath dorsal folds adjacent to buccal ganglia at rear of buccal cavity. Salivary glands (Fig. 8: sg) forming short, coiled, unbranched tubules, opening dorsolaterally alongside odontophore; salivary glands passing through circumesophageal nerve ring (Fig. 8: nr), but not extending posteriorly. Thick buccal retractors (Fig. 8: rt) extending from rear wall of buccal mass, inserting on lateral walls of cephalic hemocoel anterior to nerve ring. Nerve ring lying short distance back from posterior end of cephalic tentacles. Radular sac short, projecting slightly past end of buccal mass and curving dorsally underneath anterior esophagus. Within anterior esophagus, short, glandular midventral fold just behind odontophore. Paired ventral longitudinal folds commencing immediately behind midventral fold. Walls of anterior and midesophagus with paired, longitudinal ventral and dorsal folds and numerous additional, less prominent longitudinal grooves; dorsal and ventral folds fusing with each other (i.e., right dorsal fold with right ventral fold) at posterior end of midesophagus, enclosing shallow, weakly grooved, rear-projecting triangular troughs. Midesophageal gland lacking.

Midgut. Esophagus opening to gastric chamber floor at left (Fig. 9: e). Marginal fold (Fig. 9: mf) extending anteriorly alongside major typhlosole (Fig. 9: t1), then turning posteriorly bordering edge of sorting area (Fig. 9: sa). Sorting area rectangular, with rounded posterior margin. Marginal fold elaborated into small pad at left, posterior tip of sorting area (Fig. 9: sap). Accessory marginal fold (Fig. 9: amf) emerging from left side of esophageal aperture, paralleling marginal fold, curving anteriorly around posterior end of sorting area; accessory marginal fold bifurcate posteriorly. Epithelium of midgut floor finely grooved adjacent to major typhlosole at right of marginal fold. Midgut roof at left of sorting area deeply, irregularly creased, cuticularized (Fig. 9: cu). Gastric shield (Fig. 9: gs) large, continuous with cuticle of midgut roof and crystalline style pocket (Fig. 9: p). Broad, prominent fold bounding u-shaped depression (Fig. 9: u) below lip of style sac (Fig. 9: ss). Glandular pad (Fig. 9: gp) small, broadly rounded; accessory pad at anterior end lacking. Crescentic ridge (Fig. 9: cr) extending back from near esophageal aperture and fusing to right side of glandular pad, bounding shallow crescentic groove. Proximal tip of crescentic ridge bounding deep pouch with two digestive gland ducts. Shallow caecum (Fig. 9: c) extending ventrally under glandular pad behind gastric shield. Single, weakly developed longitudinal fold (Fig. 9: cf) behind gastric shield, opposite caecum. Style sac (Fig. 5: ss) communicating proximally with intestine. Crystalline style present.

Hindgut. Proximal intestine (Figs. 5, 6: int) passing below distal tip of style sac, then extending posteriorly alongside style sac (Figs. 5, 6: ss) to main gastric chamber (Fig. 6: sto). Intestine continuing forward, passing under posterior end of main kidney chamber (Figs. 5, 6: kd), entering pallial roof between bladder (Figs. 5, 6: b) and main kidney chamber, to papillate anus near mantle margin (Fig. 8: int).

Reno-Pericardial System: Voluminous kidney (Fig. 5: kd) extending from anterior end of main gastric chamber (Fig. 6: sto) alongside style sac and pericardium into mantle roof. Kidney lumen partially subdivided into two main chambers. Main chamber (Figs. 5, 11: kd) extending full length of kidney, surrounding pericardium dorsally and at right, anteriorly overhanging base of mantle cavity; lumen mostly occluded by excretory tubules developed in roof and along walls. Small bladder (Figs. 5, 6: b) at right of main chamber, extending into pallial roof between intestine (Fig. 5: int) and pallial gonoduct. Bladder (exposed chamber in Fig. 11) communicating with main chamber via small aperture (Fig. 11: arrow) just behind afferent renal vessel (Fig. 11: arv). Bladder partially subdivided posteriorly by incomplete horizontal septum of excretory tissue (Fig. 11: s), separating narrow triangular chamber below. Large sheet of excretory tubules branching from afferent renal vessel and extending anteriorly along bladder floor, partially separating narrow, shallow ventral chamber below. Nephridial gland absent.

Narrow, deep pericardium (Fig. 5: per) extending underneath kidney alongside style sac (Fig. 5: ss) past intestinal loop.

Nervous System: Cerebral ganglia (Fig. 10: ce) connected by short, stout commissure, each ganglion producing six nerves (optic, statocyst, tentacular, and three labial nerves). Buccal ganglia lying ventrolaterally at base of buccal mass, adjacent to retractor muscles, at outer edges of anterior esophagus. Pleural ganglia (Fig. 10: pl) lying behind and below cerebral ganglia connected to cerebral ganglia by short, thick connectives. Pedal ganglia (Fig. 10: pe) with two prominent anterior nerves and approximately five smaller accessory nerves. Statocysts (Fig. 10: st) with numerous angular statoconia present dorsally alongside pedal ganglia behind pedal connectives. Subesophageal ganglion (Fig. 10: sb) joined to left pleural ganglion by long, thick connective; connective producing one small nerve. In addition to connectives to left pleural and visceral ganglia, subesophageal ganglion producing one stout, branching nerve, one fine nerve and zygoneurous connection to right pleural ganglion (Fig. 10: z). Long connective uniting right pleural and supraesophageal ganglia (Fig. 10: sp), the latter lying at left of midesophagus (Fig. 8: sp). Dialyneury formed between pallial nerve of left pleural ganglion and osphradial nerve of supraesophageal ganglion at junction of mantle roof and floor. Single visceral ganglion present at base of cephalic hemocoel.

Female Reproductive System: Gonad (Fig. 6: ov) dorsally overlying digestive gland (Fig. 6: dg) from tip of visceral mass to posterior end of gastric chamber (Fig. 6: sto). Oviduct emerging ventrally from ovary. Renal oviduct (Figs. 12, 13: ovi) forming short recurvent loop behind mantle cavity before entering base of glandular oviduct. Pallial oviduct, with proximal albumen (Fig. 13: ag) and distal capsule glands (Figs. 12, 13: cg). Albumen gland forming rear-facing c-shaped tube at posterior end of pallial oviduct; capsule gland developed along dorsal crest of pallial oviduct. Glandular tissue of capsule gland and much of albumen gland with opposing flattened surfaces bounding morphologically dorsal gonoductal groove. Lumen of albumen gland initially crescent-shaped, deepening abruptly just before broad, rear-facing loop. Narrow vagina along anterior one third of oviduct opening to sperm gutter (Fig. 12: sg) in median lamina. Gutter leading posteriorly to short, broad spermatophore bursa (Fig. 12: spb). Ventral free edge of median lamina inner wall (Fig. 12: dashed line) fusing posteriorly above ventral channel, dorsally enclosing entrance to seminal receptacle (Fig. 12: rcs). Communication between sperm gutter and ventral channel bounded by two folds: one prominent dorsal fold along outer ventral edge of median lamina inner wall extending from anterior end of seminal groove to posterior end of bursa, dorsally bounding ventral channel, and one ventral shallow fold extending along ventral edge of vagina short distance along outer wall of bursa, to opening of seminal receptacle.

Male Reproductive Sytem: Male reproductive anatomy unknown.

Remarks: The anatomy of *Bathanalia howesi* was described by Moore (1898) and found to be so similar to *Tiphobia* that he considered no special anatomical description necessary. Nevertheless, he felt that conchological differences were adequate to erect a separate genus. It should be emphasized that he did not explicitly confirm or reject that *B. howesi* was ovoviviparous; a figure of an animal removed from the shell (pl. 12, fig. 31) did not show a uterine brood pouch, but did not specify gender. Later, Moore (1903) reiterated the similarity with *Tiphobia*, but again was silent on the point of ovoviviparity. Moore (1898) made note of the dialyneury on the right that he managed to locate with the aid of histological sections, and which could not be located in *Tiphobia*; he considered this feature to be of special significance in assessing affinities of the two.

Through incorrect and incomplete descriptions of several anatomical features (including radula, midgut, and the nervous system in particular, erroneously described comprising a concentrated nerve ring and pedal cords with cross connections) and appalling misinterpretations of these structures seen through the lens of their “unquestionable” marine affinities (Moore, 1903), Moore (1898) placed *Tiphobia* and *Bathanalia* in their own family, the Tiphobiidae with affinities to the Stromboidea. He evidently was not aware that Bourguignat (1886) had already established this family-group name to circumscribe four species of *Tiphobia*, three of which are now considered synonyms of *Tiphobia horei*.

Leloup (1953: 132, fig. 72DD) figured a spiral operculum for *Bathanalia straeleni*, and reported a rachidian with 12/1/12; lateral teeth with 5–8/1/~15; almost identical marginal teeth with ~12/~15. Leloup (1953) also reported that two juvenile shells (one empty and one containing an animal) had been recovered from the mantle cavity near the operculum of an individual of *B. straeleni* and concluded that this species is a uterine brooder. This observation, compounded by Moore's (1898) silence on this point, has formed the basis for a persistent misconception that *Bathanalia* species are ovoviviparous (e.g., Pilsbry & Bequaert, 1927; Brown, 1994; Glaubrecht, 2008). It is clear from examination of the figure in Leloup (1953: 135, fig. 73C) that the shell in question is not a juvenile *B. straeleni*, lacking the characteristic keel that develops rapidly in post-embryonic whorls (see Fig. 2), but rather is a juvenile of *Tiphobia horei* (Strong & Glaubrecht, 2007: fig. 8K, M), specimens of which were recovered from the same site (no. 50; Leloup, 1953). Consequently, the juveniles must have been drawn into the mantle cavity when the animal retracted. Female reproductive anatomy as revealed in the present investigation confirms that *B. straeleni* is not ovoviviparous as no embryos were recovered from the pallial oviduct of a sexually mature female, and the oviduct does not possess any characteristics commonly associated with uterine brooding (Strong & Glaubrecht, 2007).

Chytra kirkii
(Smith, 1880)

Material Examined: (BMNH 1880.12.21.11-14) (5 syntypes); (BMNH 1909.5.27.10-13) (4 spms); (BMNH, A.S. Kennard Colln., Acc. No. 1824) (3 spms); (BMNH) (4 spms); (BMNH 1953.8.15.248-257) (21 spms); (AMS 5493) (6 spms); (CM 62.29291) (3 spms); (DBL) (2 spms); (DBL) (1 spm); (USNM 120893) (1 spm); (USNM 149918) (1 spm); (ZMB 94.708) (4 spms); (ZMB 92.355) (3 spms). Burundi: Rumonge, 60 km S Bujumbura, 25–100 m (03°52'S, 29°23'E) (USNM 882005) (3 spms; 1 spm dissected). Democratic Republic of Congo: small bay to the south of Cape Tembwe (IRSNB no. 68) (1 spm). Tanzania: Malagarasi delta, 10–15 km from the coast, 33–17 m (IRSNB no. 63) (1 spm dissected); near Rusago (ZMB 220.155) (2 spms).

Shell: Adult shell comprising up to seven whorls, typically with broken apex (Fig. 14). Embryonic shell unknown. Teleoconch whorls flat, slightly rounded just below suture, with upturned basal keel just above suture. Teleoconch axial sculpture comprising fine sigmoidal growth lines. Early teleoconch whorls smooth, rapidly developing two fine spiral cords, soon joined by two additional spiral cords, plus one spiral cord along basal keel. Cords thickening and becoming nodulose. Single fine spiral thread appearing between each of initial four cords; spiral threads thickening and becoming nodulose on later adult teleoconch whorls. Growth lines becoming more prominent on final teleoconch whorl. Basal disk of shell sculptured with numerous, prominent nodulose spiral cords. Aperture thickened, angular but holostome. Umbilicus narrow. Shell microstructure (Fig. 15) comprising five layers from external to internal: (1) irregular, simple prismatic structure, (2) simple radial crossed lamellar structure, (3) simple comarginal crossed lamellar structure, (4) simple radial crossed lamellar structure, (5) irregular, simple prismatic structure.

External Anatomy: Operculum (Fig. 21) transparent, amber brown in color. Operculum spiral, comprising approximately 5.5 whorls, increasing evenly in size.

Foot narrowly ovate, with narrow propodium with shallow pedal gland along anterior margin (Fig. 23: ap). Columellar muscle extending to anterior end of style sac, just behind base of mantle cavity. In females, ovipositor present (Fig. 20: ovp) on right side of foot, just behind foot sole margin at junction of propodium and mesopodium. Aperture of ovipositor forming simple, oblique slit bounded by inflated folds; lumen shallow, simple, with fine grooves. Finely grooved tract to foot sole and ciliated egg groove between ovipositor and pallial oviduct both lacking.

Cephalic tentacles (Figs. 20, 23: t) smooth, long, tapering, more than twice as long as snout. Eyes located on small protuberances at base of tentacles. Snout rounded, tapering anteriorly to small mouth opening at tip.

Mantle cavity short, extending approximately one half whorl. Hypobranchial gland thin, inconspicuous (Fig. 22: hg). Mantle edge smooth. Ctenidium (Figs. 22, 23: ct) extending from near mantle margin to rear of mantle cavity; leaflets narrowly triangular. Osphradium (Fig. 23: os) smooth, short, roughly one fourth of ctenidium in length, bordered by distinct ridge at right for most of length, and at left by overhanging efferent branchial vessel.

Alimentary System: Foregut. Radula taenioglossate (Fig. 16). Rachidian (Fig. 17) squar-

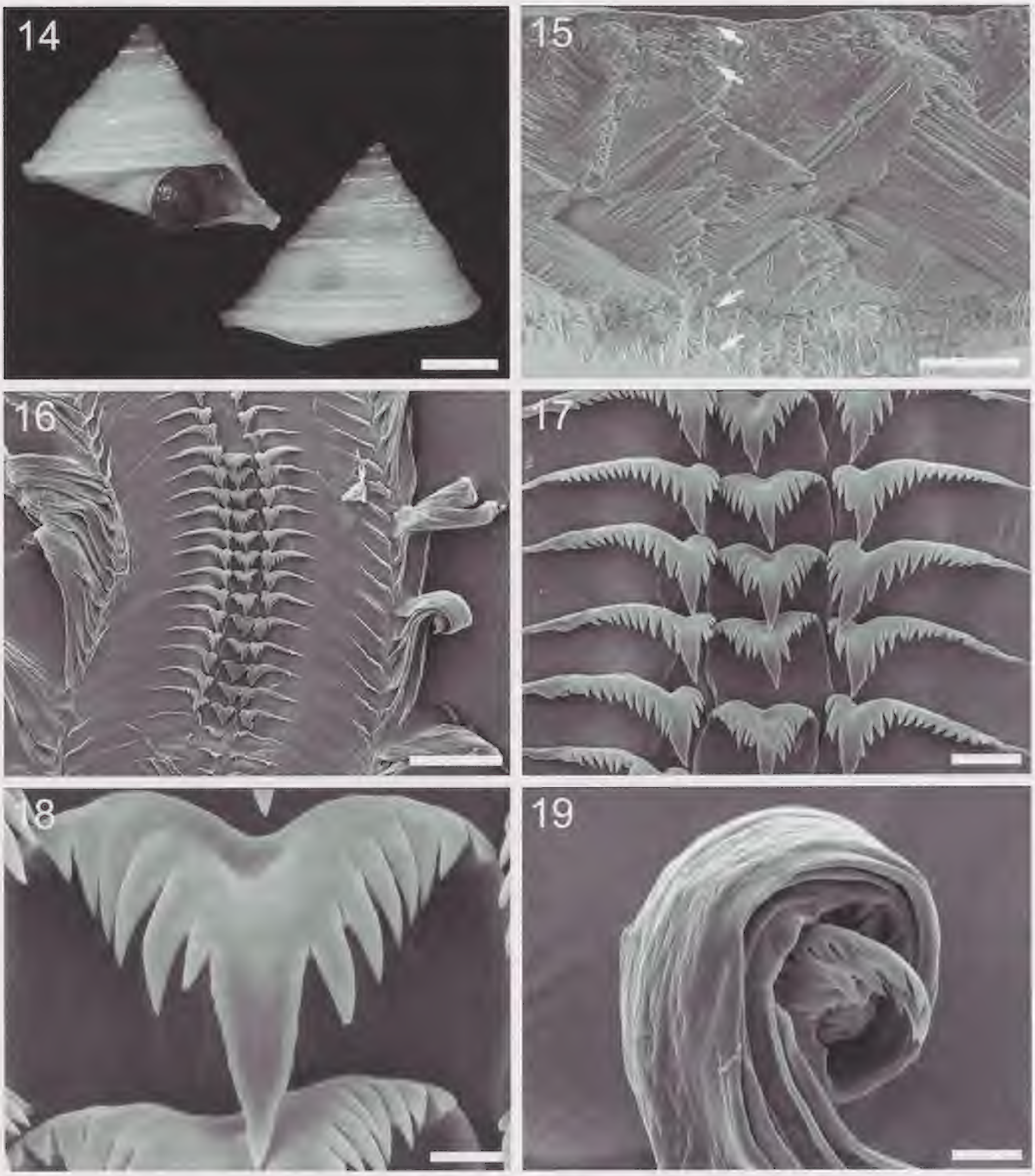

FIGS. 14–19. Shell and radula morphology of *Chytra kirkii* (IRSNB no. 63, except when noted). FIG. 14: Adult shell (IRSNB no. 68). Scale bar = 5 mm; FIG. 15: Shell microstructure. Cross section through shell parallel to aperture; outside of shell is uppermost. Order of layers from external to internal: (a) irregular, simple prismatic structure, (b) simple radial crossed lamellar structure, (c) simple comarginal crossed lamellar structure, (d) simple radial crossed lamellar structure, (e) irregular, simple prismatic structure. Arrows indicate transitions between layers. Scale bar = 50 µm; FIG. 16: Radula. Scale bar = 100 µm; FIG. 17: Rachidian and lateral teeth. Scale bar = 20 µm; FIG. 18: Rachidian tooth. Scale bar = 5 µm; FIG. 19: Marginal teeth. Scale bar = 10 µm.

ish, tapering to v-shaped lower margin. Upper margin slightly concave, with cutting edge bearing single, prominent, pointed central cusp bounded by six to eight pointed denticles on each side (Fig. 18). Lateral teeth with extremely long lateral extensions (Fig. 16),

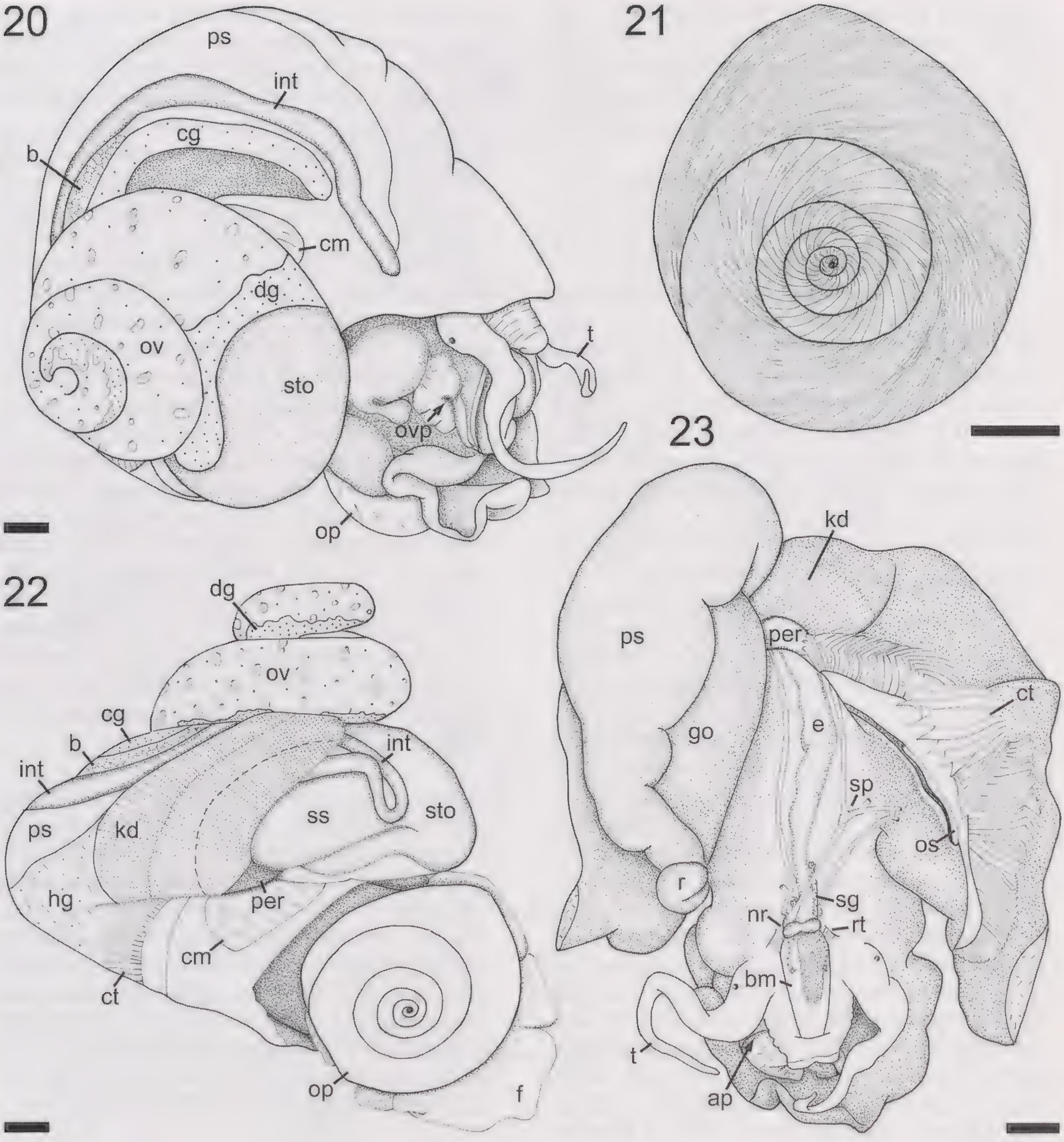

FIGS. 20–23. External anatomy of *Chytra kirkii* (IRSNB no. 63). FIG. 20: External view of organs in visceral mass; right lateral view of female head-foot with ovipositor; FIG. 21: Operculum; FIG. 22: External view of organs in visceral mass. Dashed line indicates extent of pericardium under main kidney chamber; FIG. 23: Dorsal view of mantle cavity and organs of cephalic hemocoel seen by transparency. Anterior is below. Abbreviations: ap, anterior pedal gland; b, bladder; bm, buccal mass; cg, capsule gland; cm, columellar muscle; ct, ctenidium; dg, digestive gland; e, esophagus; f, foot; go, pallial gonoduct; hg, hypobranchial gland; int, intestine; kd, kidney; nr, circumesophageal nerve ring; op, operculum; os, osphradium; ov, ovary; per, pericardium; ovp, ovipositor; ps, periintestinal sinus; r, rectum; rt, buccal retractor; sg, salivary gland; sp, supraesophageal ganglion; ss, style sac; sto, stomach; t cephalic tentacle. Scale bars = 1 mm.

roughly twice as long as cutting edge. Cutting edge with single, prominent pointed cusp flanked by five to seven inner and 9–14 outer pointed denticles. Outermost denticles of lateral teeth often fused and forming undulating, overhanging ridge. Marginal teeth (Figs. 16, 19) long, slender, with narrow, spoon-shaped tips bearing fine, pointed denticles of similar size and shape; inner marginal teeth with roughly five denticles, outer marginal teeth with roughly 8 denticles along inner edge. Precise dentition of marginal teeth could not be assessed due to curling and clumping of teeth of single available specimen.

Mouth opening ventrally at anterior end of snout. Buccal mass (Fig. 23: bm) narrow, elongate; small odontophore occupying posterior half of buccal cavity. Narrowly triangular, glandular subradular organ extending along floor of buccal cavity at anterior end of odontophore. Small, paired jaw dorsally flanking mouth at anterior ends of dorsal folds. Shallow, nonglandular buccal pouches extending underneath dorsal folds adjacent to buccal ganglia at rear of buccal cavity. Salivary glands (Fig. 23: sg) forming short, coiled tubules with branching tips, opening dorsolaterally alongside odontophore; salivary glands passing through circumesophageal nerve ring (Fig. 23: nr). Salivary glands asymmetrical with right gland terminating within nerve ring and left gland extending short distance posteriorly. Thick buccal retractors (Fig. 23: rt) extending from rear wall of buccal mass, inserting on lateral walls of cephalic hemocoel alongside nerve ring. Nerve ring lying short distance back from posterior end of cephalic tentacles. Radular sac short, projecting slightly past end of buccal mass and curving dorsally underneath anterior esophagus. Within anterior esophagus, short, glandular midventral fold just behind odontophore. Paired ventral longitudinal folds commencing immediately behind midventral fold. In single well-preserved specimen, ventral folds apparently fusing for short distance at anterior end of midesophagus and forming elevated, transverse fold, then separating and continuing through midesophagus. Walls of anterior and midesophagus with paired, longitudinal ventral and dorsal folds; dorsal and ventral folds continuing through midesophagus and continuous with folds in posterior esophagus. Posterior esophagus with numerous folds of equal height. Midesophageal gland lacking.

Midgut. Esophagus opening to gastric chamber floor at left (Fig. 24: e). Marginal fold (Fig. 24: mf) extending anteriorly alongside major typhlosole (Fig. 24: t1), then turning posteriorly bordering edge of sorting area (Fig. 24: sa). Sorting area rectangular, with rounded posterior margin. Marginal fold elaborated into small, flattenend pad at left, posterior tip of sorting area (Fig. 24: sap). Accessory marginal fold (Fig. 24: amf) emerging from left side of esophageal aperture, paralleling marginal fold, curving anteriorly around posterior end of sorting area; accessory marginal fold bifurcate posteriorly. Epithelium of midgut floor finely, regularly grooved at right of marginal fold and along projecting tip of major typhlosole. Anterior midgut roof at left of sorting area deeply, irregularly creased, cuticularized (Fig. 24: cu). Gastric shield (Fig. 24: gs) moderately large, continuous with cuticle of midgut roof and crystalline style pocket (Fig. 24: p). Glandular pad (Fig. 24: gp) large, elongate, broadly rounded; accessory pad at anterior end lacking. Crescentic ridge (Fig. 24: cr) extending back from near esophageal aperture and fusing to right side of glandular pad, bounding deep, narrow crescentic groove. Proximal crescentic ridge bounding two digestive gland ducts at left (Fig. 24: dd). Very shallow caecum (Fig. 24: c) extending ventrally under glandular pad behind gastric shield. One to two weakly developed longitudinal folds (Fig. 24: cf) behind gastric shield, opposite caecum. Style sac (Fig. 22: ss) communicating proximally with intestine). Crystalline style present.

Hindgut. Proximal intestine (Fig. 22: int) passing below distal tip of style sac, then extending posteriorly alongside style sac (Fig. 22: ss), forming broad loop over proximal style sac adjacent to main gastric chamber (Fig. 22: sto). Intestine continuing forward, passing under posterior end of main kidney chamber (Fig. 22: kd), entering pallial roof between bladder (Fig. 22: b) and main kidney chamber, to papillate anus near mantle margin (Fig. 23: r). Voluminous periintestinal sinus (Fig. 23: ps) surrounding pallial portion of intestine.

Reno-Pericardial System: Voluminous kidney (Fig. 22: kd) extending from anterior end of main gastric chamber (Fig. 22: sto) alongside style sac and pericardium into mantle roof. Kidney lumen partially subdivided into two main chambers. Main chamber (Fig. 20: kd) extending full length of kidney, surrounding pericardium dorsally and at right, anteriorly overhanging base of mantle cavity; lumen mostly occluded by excretory tubules developed in roof and along walls. Large bladder (Figs. 20, 22: b) at right of main chamber, extending into pallial roof between intestine (Figs. 20, 22: int) and pallial gonoduct (Figs. 20, 22: cg). Bladder communicating with main chamber via small aperture just behind affer-

24

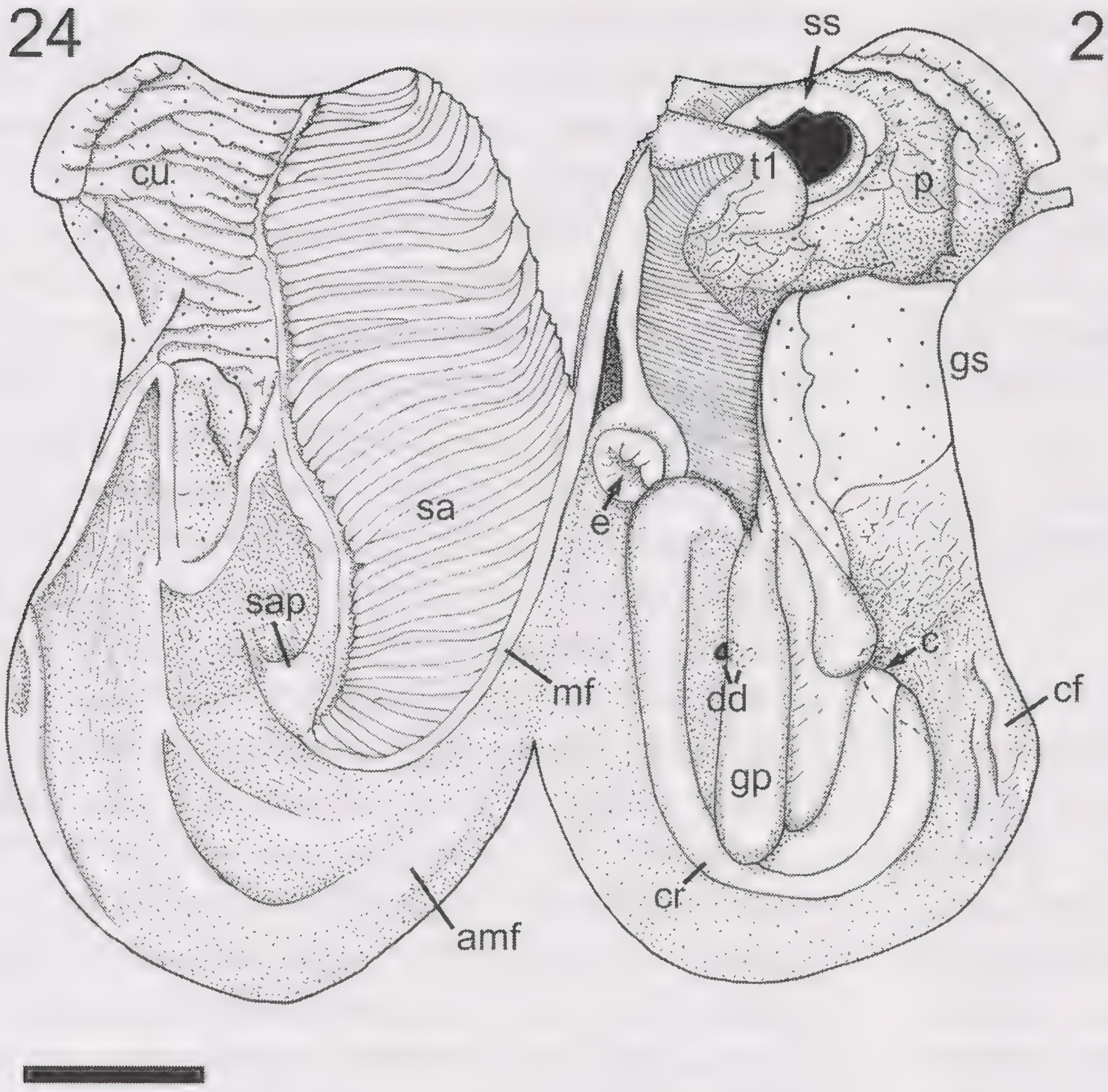

25

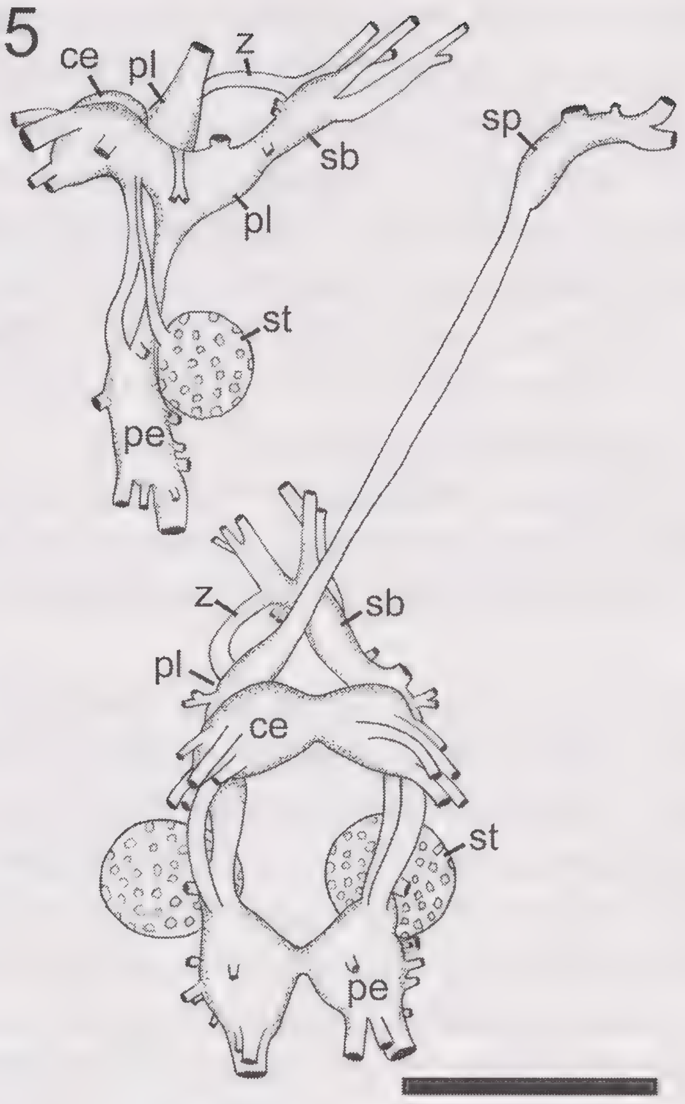

26

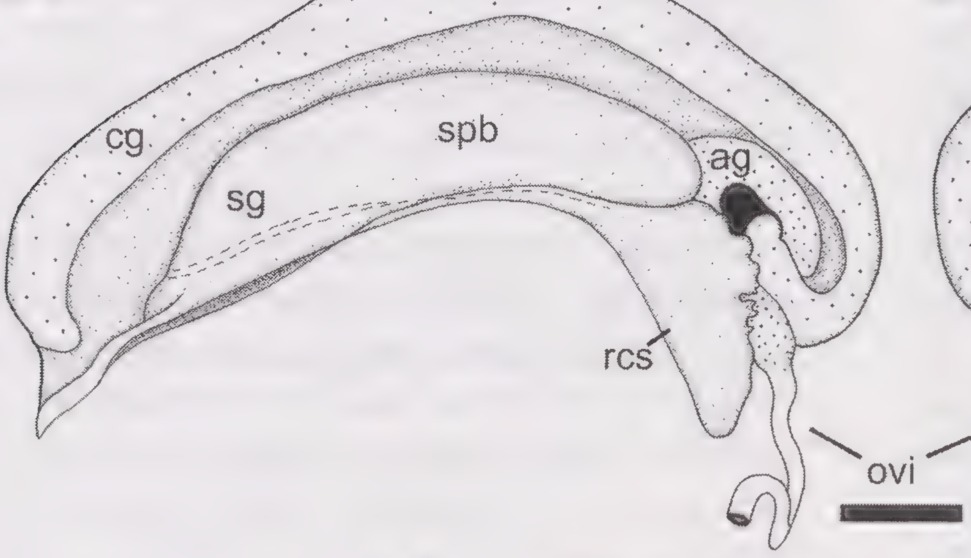

27

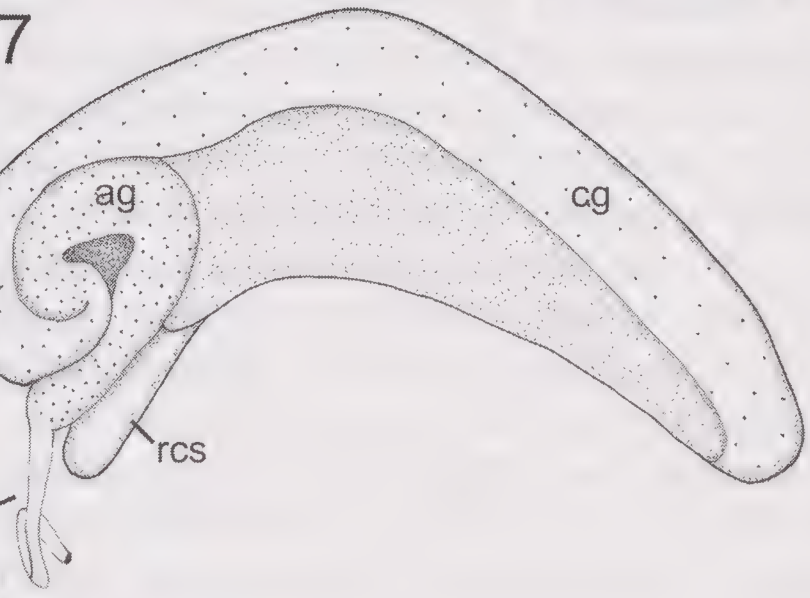

28

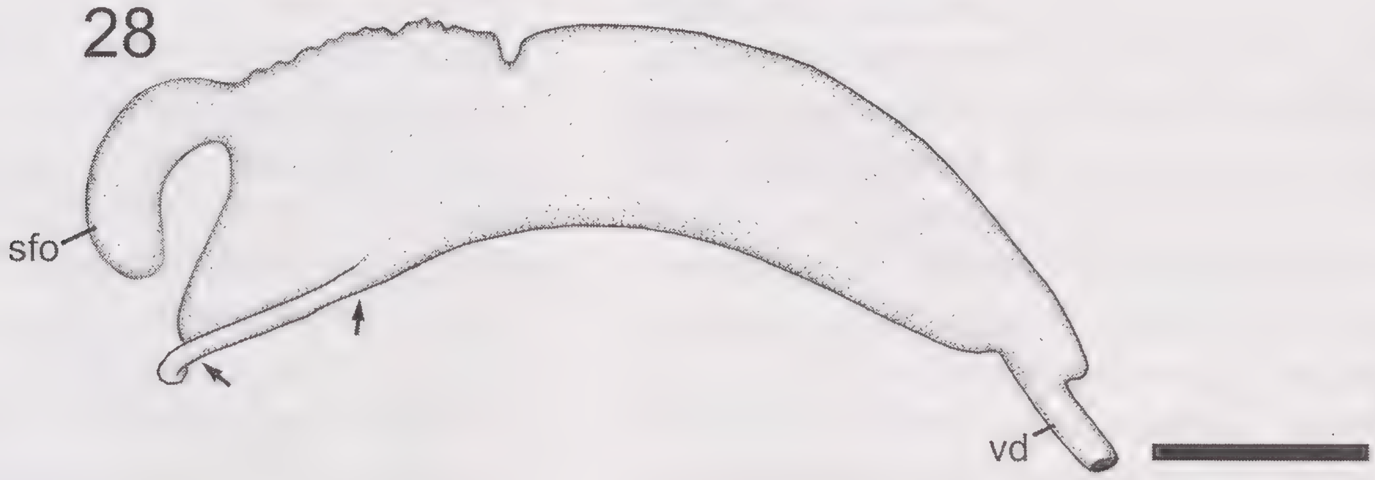

FIGS. 24–28. Internal anatomy of *Chytra kirkii* (IRSNB no. 63, except when noted). FIG. 24: Midgut anatomy. Dorsal view, anterior is uppermost; FIG. 25: Circumesophageal nerve ring. Left lateral view (above) and frontal view (below); FIG. 26: External, left lateral view of pallial oviduct. Anterior is at left. Double dashed line indicates opening from bursa to gonoductal groove; single dashed line indicates continuation of inner edge of medial lamina as shallow groove to opening of seminal receptacle; FIG. 27: External, right lateral view of pallial oviduct. Anterior is at right; FIG. 28: External, left lateral view of prostate (USNM 882005). Anterior is at left. Arrows indicate extent of opening to gonoductal groove. Prominent grooves of lateral lamina seen by transparency. Abbreviations: ag, albumen gland; amf, accessory marginal fold; c, caecum; ce, cerebral ganglion; cf, caecal fold; cg, capsule gland; cr, crescentic ridge; cu, cuticularized region in midgut roof; dd, digestive gland duct; e, esophagus; gp, glandular pad; gs, gastric shield; mf, marginal fold; ovi, renal oviduct; p, crystalline style pocket; pe, pedal ganglion; pl, pleural ganglion; rcs, seminal receptacle; sa, sorting area; sb, subesophageal ganglion; sap, sorting area pad; sfo, spermatophore forming organ; sg, seminal groove; sp, supraesophageal ganglion; spb, spermatophore bursa; ss, style sac; st, statocyst; t1, major typhlosole; vd, vas deferens; z, zygoneury. Scale bars = 1 mm.

ent renal vessel. Bladder partially subdivided posteriorly by incomplete horizontal septum of excretory tissue, separating short, broad chamber below. Large sheet of excretory tubules branching from afferent renal vessel and extending anteriorly along bladder floor. Excretory tissue in bladder highly developed along floor and roof, mostly occluding lumen. Nephridial gland absent.

Narrow, deep pericardium (Fig. 22: per) extending underneath kidney alongside style sac (Fig. 22: ss) to intestinal loop.

Nervous System: Cerebral ganglia (Fig. 25: ce) connected by short, stout commissure, each ganglion producing six nerves (optic, statocyst, tentacular, and three labial nerves). Buccal ganglia lying ventrolaterally at base of buccal mass, at inner edge of retractor muscles, below anterior esophagus. Pleural ganglia (Fig. 25: pl) lying behind and below cerebral ganglia connected to cerebral ganglia by short, thick connectives. Pedal ganglia (Fig. 25: pe) with two prominent anterior nerves and approximately seven to eight smaller accessory nerves. Statocysts (Fig. 25: st) with numerous angular statoconia present dorsally alongside pedal ganglia behind pedal connectives. Subesophageal ganglion (Fig. 25: sb) joined to left pleural ganglion by long, thick connective; connective producing one small nerve. In addition to connectives to left pleural and visceral ganglia, subesophageal ganglion producing one stout, branching nerve, one finer branching nerve, two small accessory nerves and zygoneurous connection to right pleural ganglion (Fig. 25: z). Very long connective uniting right pleural and supraesophageal ganglia (Fig. 25: sp), the latter lying at left of cephalic hemocoel, well back from circumesophageal nerve ring (Fig. 23: sp). Dialyneury formed between pallial nerve of left pleural ganglion and osphradial nerve of supraesophageal ganglion at junction of mantle roof and floor. Single visceral ganglion present at base of cephalic hemocoel.

Female Reproductive System: Gonad (Fig. 20: ov) dorsally overlying digestive gland (Fig. 20: dg) from tip of visceral mass to posterior end of gastric chamber (Fig. 20: sto). Oviduct emerging ventrally from ovary. Renal oviduct (Figs. 26, 27: ovi) forming short recurvent loop behind mantle cavity before entering base of glandular oviduct. Pallial oviduct, with proximal albumen (Figs. 26, 27: ag) and distal capsule glands (Figs. 26, 27: cg). Albumen gland forming rear-facing c-shaped tube at posterior end of pallial oviduct; capsule gland developed along dorsal crest of pallial oviduct. Glandular tissue of capsule gland and much of albumen gland with opposing flattened surfaces bounding morphologically dorsal gonoductal groove. Lumen of albumen gland initially crescent-shaped, deepening abruptly just before broad, rear-facing loop. Narrow vagina along anterior one third of oviduct opening to sperm gutter (Fig. 26: sg) in median lamina. Gutter leading posteriorly to elongate, narrow spermatophore bursa (Fig. 26: spb). Inner wall of median lamina fusing to outer wall, restricting communication between spermatophore bursa and ventral channel to short, anterior slit (Fig. 26: double dashed line). Ventral edge of median lamina inner wall (Fig. 26: single dashed line) continuing posteriorly as shallow groove above ventral channel, posteriorly enclosing entrance to seminal receptacle (Fig. 26: rcs). Communication between sperm gutter and ventral channel bounded by shallow fold extending along ventral edge of vagina.

Male Reproductive System: Single immature specimen available. Narrow vas deferens (Fig. 28: vd) emerging ventrally from testes, entering posterior end of prostate at base of mantle cavity. Prostate glandular, forming flattened tube, opening to mantle cavity through narrow, ventral slit along anterior one fourth to one fifth (arrows). Posterior two thirds of prostate separated from anterior third by slight dorsal constriction. Glands of posterior lateral lamina dorsally deeply longitudinally grooved; anterior portion of lateral lamina with deep oblique trough extending ventrally from dorsal constriction to above anterior end of aperture. Posterior medial lamina more weakly and irregularly longitudinally grooved; anterior medial lamina rather smooth with oblique, rear facing fine grooves along dorsal undulating ridge. Dorsal, anterior portion of prostate forming short, glandular, tube-like spermatophore-forming organ (Fig. 28: sfo). Organ terminating blindly anteriorly, communicating posteriorly with gonoductal groove via narrow aperture.

Remarks: The anatomy was described by Digby (1902), who provided accurate if not detailed descriptions of the operculum, mantle cavity (with short osphradium), radula (with considerably more denticles on the marginal teeth), midgut (with crescentic ridge and glandular pad interpreted as a spiral caecum), and nervous system (with dialyneury on the left, and zygoneury on the right, statocysts with numerous statoconia). As was typical of the time, female reproductive anatomy was described simply as a uterus. It is likely that Digby (1902) misinterpreted male reproductive anatomy for female, given the similarity of a putatively female pallial gonoduct (pl. 39, fig. 12) to a male prostate with spermatophore forming organ (as "accessory genital gland"). Digby (1902) concluded the species to be an ancestor of the Hipponicidae and Capulidae. Moore (1903) reproduced parts of Digby's (1902) description, and featured an operculum and one row of the radula.

Leloup figured (1953: 132, fig. 72Z) a spiral operculum, and reported the radula with a rachidian broader than tall, with 7–13/1/7–13; lateral teeth with 3–5/1/10–13; similar marginal teeth with 12–19/9–15. Riedel (1993) provided a description of the embryonic shell, including SEM micrographs (fig. 22; pl. 4, figs. 7, 8), showing the great similarity with the embryonic shell of *Limnotrochus* (Figs. 30–32); the two differing primarily in the ornament of the early teleoconch. West & Cohen (1996) reported four layers of crossed lamellar microstructure in the shell.

Limnotrochus thomsoni
Smith, 1880

Material Examined: (BMNH 1880.12.20.45-8) (4 syntypes); (AMS C.5492) (3 spms); (BMNH, A.S. Kennard Colln., Acc. No. 1824) (2 spms); (BMNH 89.6.3.20-1) (3 spms); (BMNH 1953.8.15.235-37) (3 spms); (NHMB 830a) (18 spms); (NHMB 830b) (2 spms); (USNM 127173) (2 spms); ZMB 35243 (2 spms); ZMB 220.162 (2 spms); (MRAC) (3 spms); (ZMB 35243). Burundi: Rumonge, 60 km S Bujumbura, 25–100 m (03°52'S, 29°23'E) (USNM 882015) (6 spms); Nyanza-Lac, 35–40 ft (04°20'S, 29°36'E) (USNM 857904) (1 spm). Democratic Republic of Congo: (DBL) (1 spm); Kalemie (BMNH) (2 spms); same (USNM 341838) (1 spm). Tanzania: beach S of Karema (ZMB 220.031) (3 spms); Kigoma (BMNH 1920.10.26.199) (1 spm); near Rusago (ZMB 220.032) (1 spm); Uva Island, near Kassanga (ZMB 52268) (1 spm). Zambia: Chipata Bay, 80 m (08°41.700'S, 31°08.952'E) (ZMB 220.162) (2 spms); Kasakalawe, 4–5 m (08°47.480'S, 31°04.494'E) (ZMB 220.087) (2 spms); Kasenga Point, 2 m (08°42.887'S, 31°08.476'E) (ZMB 220.025) (1 spm); Kombe (08°47.52'S, 31°01.11'E) (ZMB 107.056) (1 spm); same (ZMB 107.057) (1 spm); same (ZMB 107.058) (1 spm); same (ZMB 107.059) (1 spm); same (ZMB 107.060) (1 spm dissected); same (ZMB 107.102) (9 spms); Kumbula Island, 21 m (08°45.258'S, 31°05.116'E) (ZMB 220.038) (1 spm dissected); Mpulungu Field Station, 6 m (08°45.992'S, 31°06.402'E) (ZMB 220.065) (2 spms; 1 spm dissected); Mpulungu (DBL) (2 spms); same, 30 m (DBL) (6 spms).

Shell: Adult shell comprising up to six whorls, typically with broken apex (Fig. 29). Apical cap of embryonic shell with irregularly, finely textured surface, rapidly giving way to numerous fine spiral threads (Fig. 32). Gradual transition to teleoconch marked by development of smooth, sigmoidally curved, opisthocyrt axial threads, undulating peripheral keel at shoulder and prominent spiral cord below keel at suture (Fig. 31). By third teleoconch whorl, spiral threads becoming obsolete and one additional spiral cord appearing between keel and basal cord, visible on flattened basal portion of whorl. By sixth teleoconch whorl, additional spiral threads appearing, producing reticulate pattern on upper portion and sides of whorl; three to four prominent cords appearing on basal portion of whorl producing undulating lower surface (Fig. 30). By sixth whorl, keel developing nodulose sculpture. On subsequent teleoconch whorls, three nodulose cords appearing above keel, appearing in order from most prominent below suture, to least prominent just above keel; cord at suture and cords on base becoming nodulose. Aperture thickened, with weakly developed posterior siphon. Umbilicus narrow. Shell microstructure (Fig. 33) comprising six layers from external to internal: (1) irregular, simple prismatic structure, (2) simple radial crossed lamellar structure, (3) simple comarginal crossed lamellar structure, (4) simple radial crossed lamellar structure, (5) irregular, complex crossed lamellar structure, (6) irregular, simple prismatic structure.

External Anatomy: Operculum (Fig. 35) transparent, amber brown in color. Operculum weakly paucispiral, comprising approximately 4.5 whorls. Initial four whorls increasing gradually in diameter; final one half whorl expanding rapidly, increasing roughly twice in diameter.

Foot narrowly ovate, with narrow propodium bearing shallow pedal gland along anterior

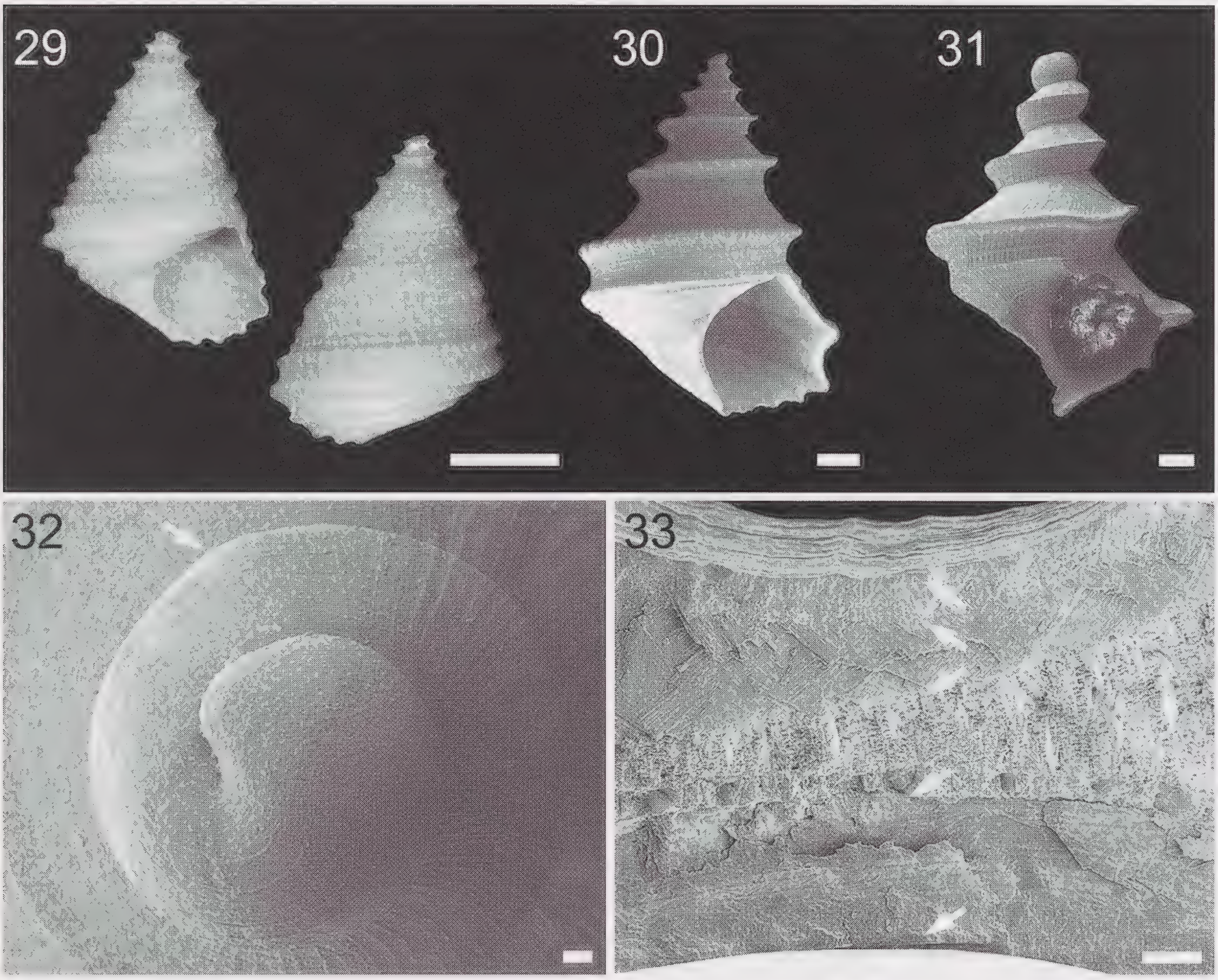

FIGS. 29–33. Shell morphology of *Limnotrochus thomsoni*. FIG. 29: Adult shell (ZMB 107.102). Scale bar = 5 mm; FIG. 30: Shell of sub-adult (DBL). Scale bar = 1 mm; FIG. 31: Juvenile shell (DBL). Scale bar = 200 µm; FIG. 32: Embryonic shell (DBL), apical view. Arrow indicates approximate transition to teleoconch. Scale bar = 20 µm; FIG. 33: Shell microstructure (ZMB 220.038). Cross section through shell parallel to aperture; outside of shell is uppermost. Order of layers from external to internal: (a) irregular, simple prismatic structure, (b) simple radial crossed lamellar structure, (c) simple comarginal crossed lamellar structure, (d) simple radial crossed lamellar structure, (e) irregular, complex crossed lamellar structure, (f) irregular, simple prismatic structure. Arrows indicate transitions between layers. Scale bar = 100 µm.

margin (Fig. 36: ap). Columellar muscle extending to style sac, just behind base of mantle cavity. In females, ovipositor present on right side of foot, just behind foot sole margin at junction of propodium and mesopodium. Aperture of ovipositor forming simple, oblique slit bounded by low folds; lumen shallow, simple. Finely grooved tract to foot sole and ciliated egg groove between ovipositor and pallial oviduct both lacking.

Cephalic tentacles (Fig. 37: t) smooth, short, triangular, slightly less than snout in length. Eyes located on small protuberances at base of tentacles. Snout rounded, tapering anteriorly to small mouth opening at tip.

Mantle cavity short, extending approximately one half whorl. Hypobranchial gland thin, inconspicuous. Mantle edge smooth. Ctenidium (Figs. 34, 36, 37: ct) extending from near mantle margin to rear of mantle cavity; leaflets broadly triangular. Osphradium (Figs. 36, 37: os) smooth, short, roughly one third of ctenidium in length, bordered by distinct ridge at right for most of length, and at left by overhanging efferent branchial vessel.

Alimentary System: Foregut. Radula taenioglossate (Fig. 38). Rachidian (Fig. 39) rectangular, wider than tall, tapering to v-

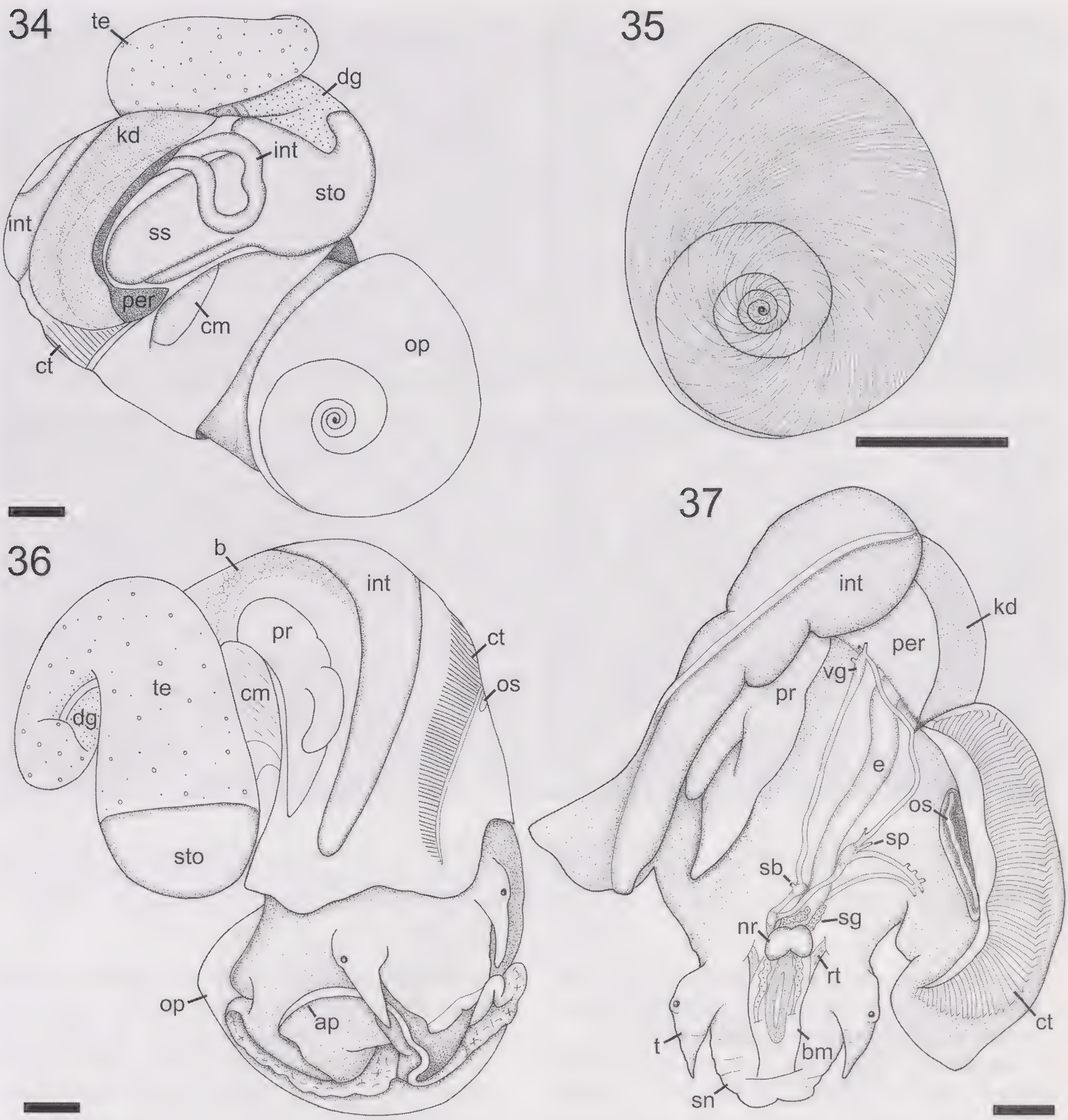

FIGS. 34–37. External anatomy of *Limnotrochus thomsoni* (ZMB 220.065). FIG. 34: External view of organs in visceral mass. Dashed line indicates extent of pericardium under main kidney chamber; FIG. 35: Operculum; FIG. 36: External view of organs in visceral mass; FIG. 37: Dorsal view of mantle cavity and organs of cephalic hemocoel seen by transparency. Anterior is below. Abbreviations: ap, anterior pedal gland; b, bladder; bm, buccal mass; cm, columellar muscle; ct, ctenidium; dg, digestive gland; e, esophagus; int, intestine; kd, kidney; nr, circumesophageal nerve ring; op, operculum; os, osphradium; per, pericardium; pr, prostate; rt, buccal retractor; sb, subesophageal ganglion; sg, salivary gland; sn, snout; sp, supraesophageal ganglion; ss, style sac; sto, stomach; t cephalic tentacle; te, testis; vg, visceral ganglion. Scale bars = 1 mm.

shaped lower margin. Upper margin slightly concave, with cutting edge bearing single, prominent, pointed central cusp bounded by 9–13 fine, pointed denticles on each side (Fig. 40). Lateral teeth with extremely long lateral extensions (Fig. 38), roughly twice as long as cutting edge. Cutting edge with single, prominent pointed cusp flanked by six to seven inner and 16–20 outer pointed denticles. Outermost denticles of lateral teeth often fused and forming undulating, overhanging ridge. Marginal teeth (Figs. 38, 41)

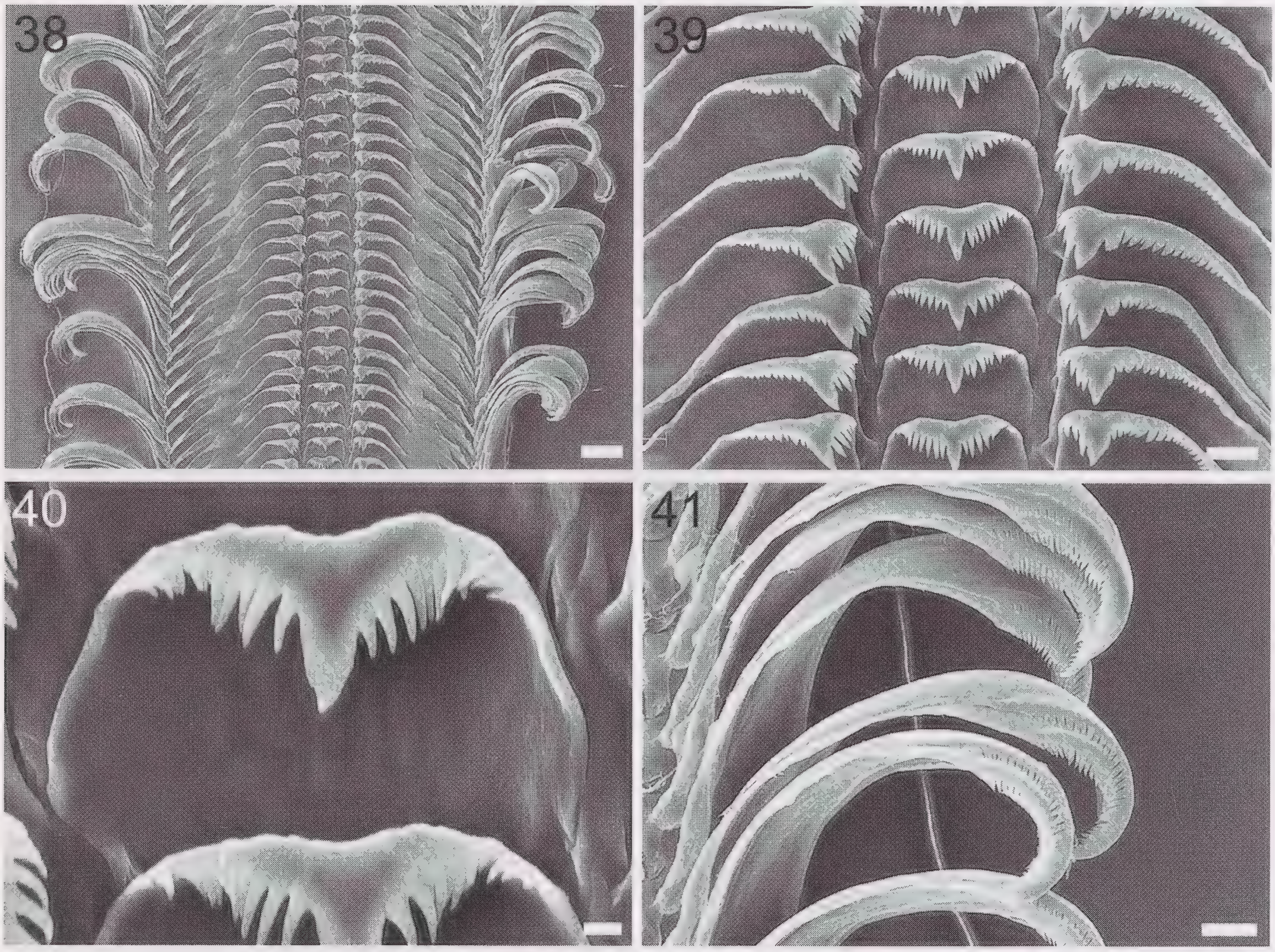

FIGS. 38–41. Radula morphology of *Limnotrochus thomsoni*. FIG. 38: Radula (ZMB 220.038). Scale bar = 30 µm; FIG. 39: Rachidian and lateral teeth (ZMB 220.038). Scale bar = 10 µm; FIG. 40: Rachidian tooth (ZMB 220.038). Scale bar = 2 µm; FIG. 41: Marginal teeth (ZMB 220.038). Scale bar = 10 µm.

long, slender, with narrow, elongate, rounded tips bearing ~28–32 fine, pointed denticles of similar size and shape along inner edge.

Mouth opening ventrally at anterior end of snout. Buccal mass (Fig. 37: bm) narrow, elongate; small odontophore occupying posterior half of buccal cavity. Narrowly triangular, glandular subradular organ extending along floor of buccal cavity at anterior end of odontophore. Small, paired jaw dorsally flanking mouth at anterior ends of dorsal folds. Shallow, nonglandular buccal pouches extending underneath dorsal folds adjacent to buccal ganglia at rear of buccal cavity. Salivary glands (Fig. 37: sg) forming long, highly convoluted tubules with grape-like branching tips, opening dorsolaterally alongside odontophore; salivary glands passing through circumesophageal nerve ring (Fig. 37: nr) and extending short distance posteriorly. Thick buccal retractors (Fig. 37: rt) extending from rear wall of buccal mass, inserting on lateral walls of cephalic hemocoel alongside nerve ring. Nerve ring lying near base of cephalic tentacles. Radular sac short, projecting slightly past end of buccal mass and curving dorsally underneath anterior esophagus. Within anterior esophagus, short, glandular midventral fold just behind odontophore. Paired ventral longitudinal folds commencing immediately behind midventral fold. Walls of anterior and midesophagus with paired, longitudinal ventral and dorsal folds; dorsal and ventral folds continuing through midesophagus and continuous with folds in posterior esophagus. Posterior esophagus with numerous folds of equal height. Midesophageal gland lacking.

Midgut. Esophagus opening to gastric chamber floor at left (Fig. 42: e). Marginal fold (Fig. 42: mf) extending anteriorly alongside major typhlosole (Fig. 42: t1), then turning posteriorly bordering edge of sorting area (Fig. 42:

42

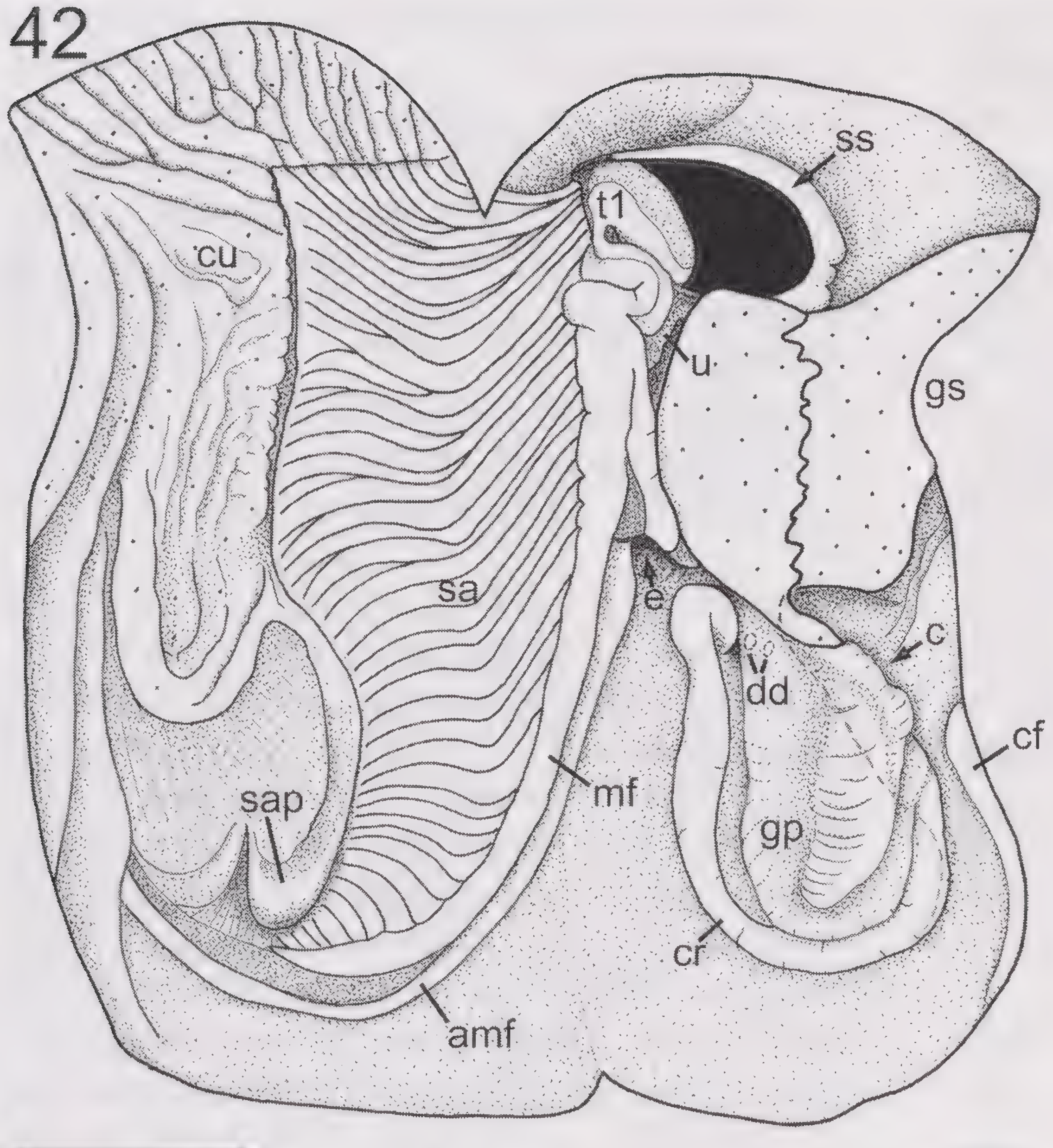

43

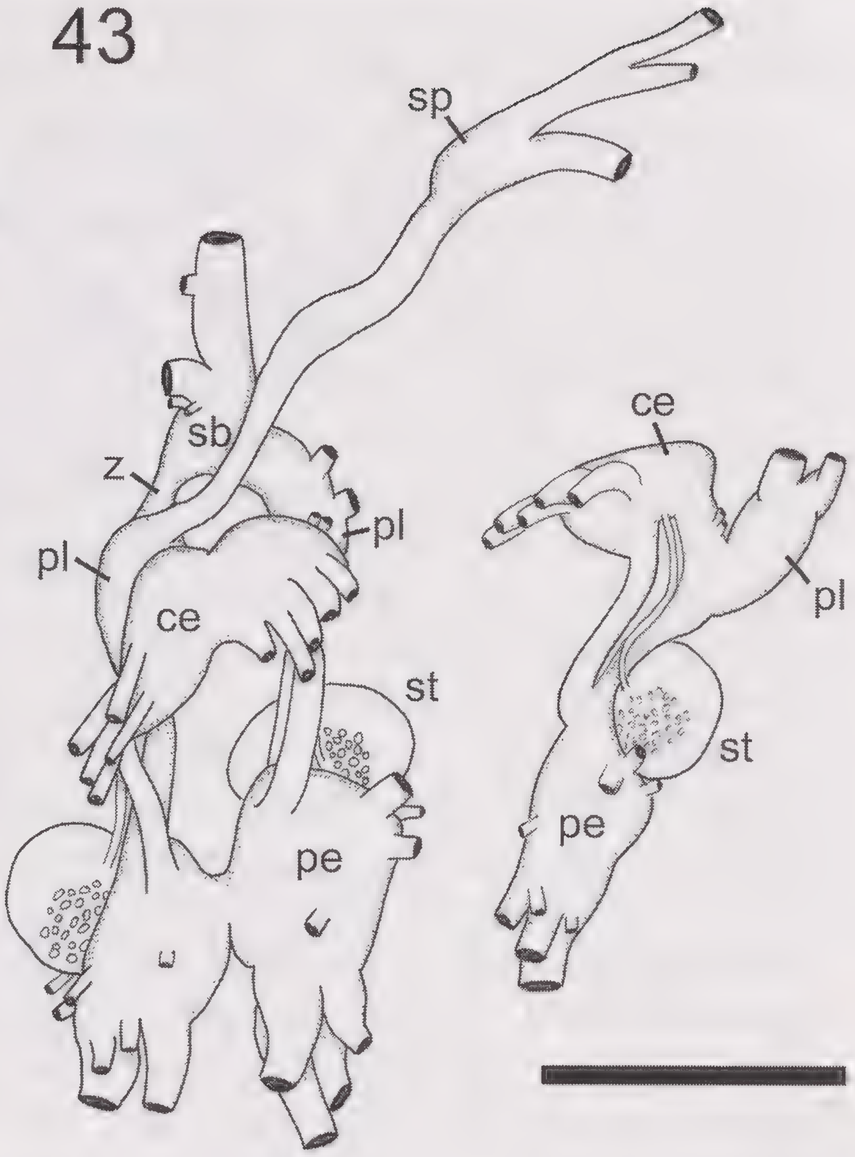

44

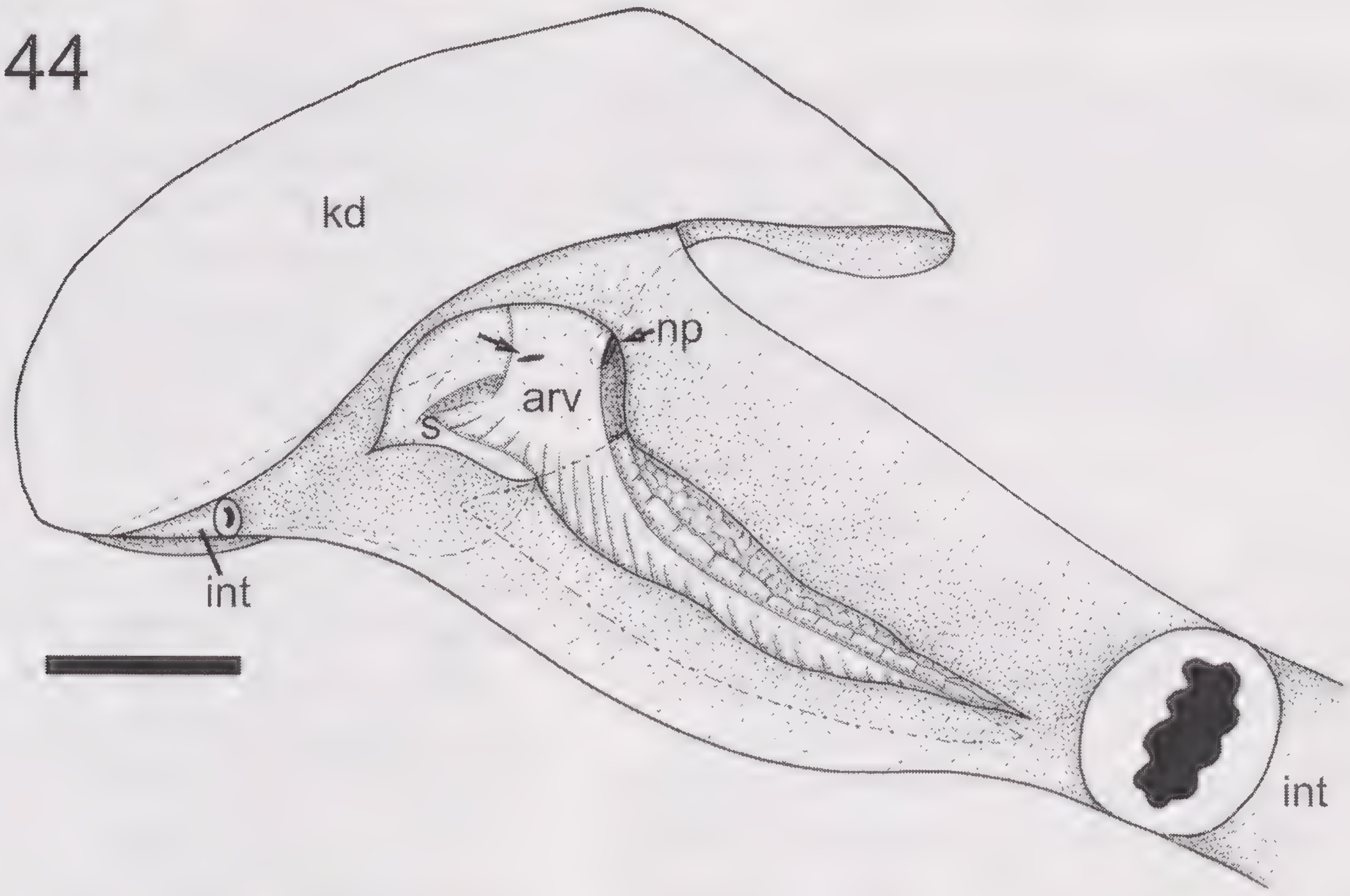

FIGS. 42–44. Internal anatomy of *Limnotrochus thomsoni* (ZMB 220.065, except when noted). FIG. 42: Midgut anatomy (ZMB 220.038). Dorsal view, anterior is uppermost; FIG. 43: Circumesophageal nerve ring. Frontal view (left) and left lateral view (right); FIG. 44: Kidney anatomy. Internal view of bladder. Lateral view, anterior is at right. Roof of bladder (below intestine) cut open to reveal interior. Abbreviations: amf, accessory marginal fold; arv, afferent renal vessel; c, caecum; ce, cerebral ganglion; cf, caecal fold; cr, crescentic ridge; cu, cuticularized region in midgut roof; dd, digestive gland duct; e, esophagus; gp, glandular pad; gs, gastric shield; int, intestine; kd, kidney; mf, marginal fold; np, nephropore; pe, pedal ganglion; pl, pleural ganglion; s, septum; sa, sorting area; sb, subesophageal ganglion; sap, sorting area pad; sp, supraesophageal ganglion; ss, style sac; st, statocyst; t1, major typhlosole; u, u-shaped fold; z, zygoneury. Scale bars = 1 mm.

sa). Sorting area rectangular, with rounded posterior margin. Marginal fold elaborated into small, crescentic pad at left, posterior tip of sorting area (Fig. 42: sap). Accessory marginal fold (Fig. 42: amf) emerging from left side of esophageal aperture, paralleling marginal fold, curving anteriorly around posterior end of sorting area; accessory marginal fold bifurcate posteriorly. Midgut roof at left of sorting area deeply, irregularly creased, cuticularized (Fig. 42: cu). Gastric shield (Fig. 42: gs) large, continuous with cuticle of midgut roof and crystalline style pocket. Prominent fold bounding narrow depression (Fig. 42: u) below lip of style sac (Fig. 42: ss). Glandular pad (Fig. 42: gp) large, elongate, broadly rounded; accessory pad at anterior end lacking. Crescentic ridge (Fig. 42: cr) extending back from near esophageal aperture and fusing to right side of glandular pad, bounding deep, narrow crescentic groove. Proximal tip of crescentic ridge bounding deep pouch with two digestive gland ducts. Elongate, shallow caecum (Fig. 42: c) extending ventrally under glandular pad behind gastric shield. Single, elongate longitudinal fold (Fig. 42: cf) behind gastric shield, opposite caecum and glandular pad. Style sac (Fig. 34: ss) communicating proximally with intestine. Crystalline style present.

Hindgut. Proximal intestine (Fig. 34: int) passing below distal tip of style sac, then extending posteriorly alongside style sac (Fig. 34: ss), forming broad loop over proximal style sac adjacent to main gastric chamber (Fig. 34: sto). Intestine continuing forward, passing under posterior end of main kidney chamber (Fig. 34: kd), entering pallial roof between bladder (Fig. 36: b) and main kidney chamber, to papillate anus near mantle margin (Fig. 37: int). Rather voluminous periintestinal sinus surrounding pallial portion of intestine.

Reno-Pericardial System: Voluminous kidney (Fig. 34: kd) extending from anterior end of main gastric chamber (Fig. 34: sto) alongside style sac and pericardium into mantle roof. Kidney lumen partially subdivided into two main chambers. Main chamber (Figs. 34, 44: kd) extending full length of kidney, surrounding pericardium dorsally and at right, anteriorly overhanging base of mantle cavity; lumen mostly occluded by excretory tubules developed in roof and along walls. Large bladder (Fig. 36: b) at right of main chamber, extending into pallial roof between intestine (Fig. 36: int) and pallial gonoduct (Fig. 36: pr). Bladder (exposed chamber in Fig. 44) communicating with main chamber via small aperture (Fig. 44: arrow) just behind afferent renal vessel (Fig. 44: arv). Bladder partially subdivided posteriorly by incomplete horizontal septum of excretory tissue (Fig. 44: s), separating elongate chamber below. Large sheet of excretory tubules branching from afferent renal vessel and extending anteriorly along bladder floor, partially separating shallow ventral chamber below. Nephridial gland absent.

Narrow, deep pericardium (Fig. 34: per) extending underneath kidney alongside style sac (Fig. 34: ss) to intestinal loop.

Nervous System: Cerebral ganglia (Fig. 43: ce) separated by slight constriction, each ganglion producing six nerves (optic, statocyst, tentacular, and three labial nerves). Buccal ganglia lying ventrolaterally at base of buccal mass, at inner edge of retractor muscles, below anterior esophagus. Pleural ganglia (Fig. 43: pl) lying behind and below cerebral ganglia connected to cerebral ganglia by short, thick connectives; left connective producing two small nerves. Pedal ganglia (Fig. 43: pe) with two prominent anterior nerves and approximately six smaller accessory nerves. Statocysts (Fig. 43: st) with numerous angular statoconia present dorsally alongside pedal ganglia behind pedal connectives. Subesophageal ganglion (Fig. 43: sb) joined to left pleural ganglion by short, thick connective; connective producing one stout nerve. In addition to connectives to left pleural and visceral ganglia, subesophageal ganglion producing one stout, branching nerve, two fine accessory nerves and zygoneurous connection to right pleural ganglion (Fig. 43: z). Long connective uniting right pleural and supraesophageal ganglia (Fig. 43: sp), the latter lying at left of midesophagus (see Fig. 37: sp). Dialyneury formed between pallial nerve of left pleural ganglion and osphradial nerve of supraesophageal ganglion at junction of mantle roof and floor. Single visceral ganglion present at base of cephalic hemocoel (Fig. 37: vg).

Female Reproductive System: Gonad (Fig. 36: te) dorsally overlying digestive gland (Fig. 36: dg) from tip of visceral mass to posterior end of gastric chamber (Fig. 36: sto). Oviduct emerging ventrally from ovary. Renal oviduct (Figs. 45, 46: ovi) entering glandular oviduct at base of mantle cavity. Pallial oviduct, with proximal albumen (Figs. 45, 46: ag) and distal capsule glands (Figs. 45, 46: cg). Albumen gland forming rear-facing c-shaped tube

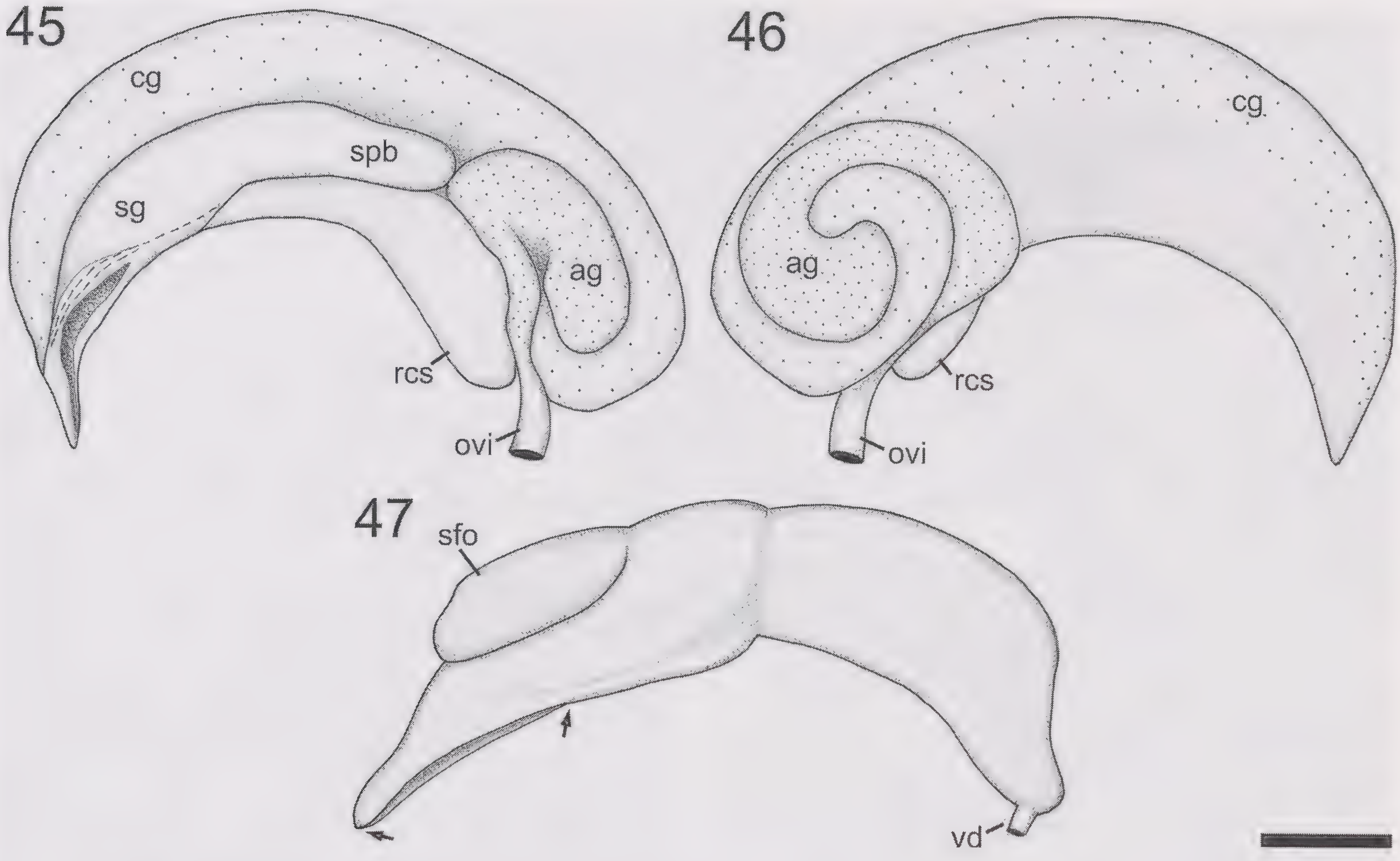

FIGS. 45–47. Reproductive anatomy of *Limnotrochus thomsoni* (ZMB 220.038, except when noted). FIG. 45: External, left lateral view of pallial oviduct. Anterior is at left. Double dashed line indicates opening from bursa to gonoductal groove; single dashed line indicates continuation of inner edge of medial lamina as shallow groove to opening of seminal receptacle; FIG. 46: External, right lateral view of pallial oviduct. Anterior is at right; FIG. 47: External, left lateral view of prostate (ZMB 220.065). Anterior is at left. Arrows indicate extent of opening to gonoductal groove. Prominent grooves of lateral lamina seen by transparency. Abbreviations: ag, albumen gland; cg, capsule gland; ovi, renal oviduct; rcs, seminal receptacle; sfo, spermatophore forming organ; sg, seminal groove; spb, spermatophore bursa; vd, vas deferens. Scale bar = 1 mm.

at posterior end of pallial oviduct; capsule gland developed along dorsal crest of pallial oviduct. Glandular tissue of capsule and albumen glands with opposing flattened surfaces bounding morphologically dorsal gonoductal groove. Narrow vagina along anterior one fourth of oviduct opening to sperm gutter (Fig. 45: sg) in median lamina. Gutter leading posteriorly to elongate, narrow spermatophore bursa (Fig. 45: spb). Inner wall of median lamina fusing to outer wall, restricting communication between spermatophore bursa and gonoductal groove to short, anterior slit (Fig. 45: double dashed line). Ventral edge of median lamina inner wall (Fig. 45: single dashed line) continuing posteriorly as shallow groove above ventral channel, posteriorly enclosing entrance to seminal receptacle (Figs. 45, 46: rcs). Communication between sperm gutter and ventral channel bounded by shallow fold extending along ventral edge of vagina.

Male Reproductive System: Narrow vas deferens (Fig. 47: vd) emerging ventrally from testes (Figs. 34, 36: te), entering posterior end of prostate at base of mantle cavity. Short distal portion of vas deferens thickened and forming straight seminal vesicle. Prostate glandular, forming flattened tube, opening to mantle cavity through narrow, ventral slit along anterior one third (arrows). Posterior half of prostate separated from anterior half by slight dorsal constriction. Glands of posterior lateral lamina deeply longitudinally grooved. Posterior medial lamina more weakly and irregularly longitudinally grooved. Dorsal, anterior portion of prostate forming short, thick, glandular, tube-like spermatophore-forming organ (Fig. 47: sfo). Organ terminating blindly anteriorly, communicating posteriorly with gonoductal groove via narrow aperture.

Remarks: The anatomy was also described by Digby (1902) who, as for *Chytra*, provided a

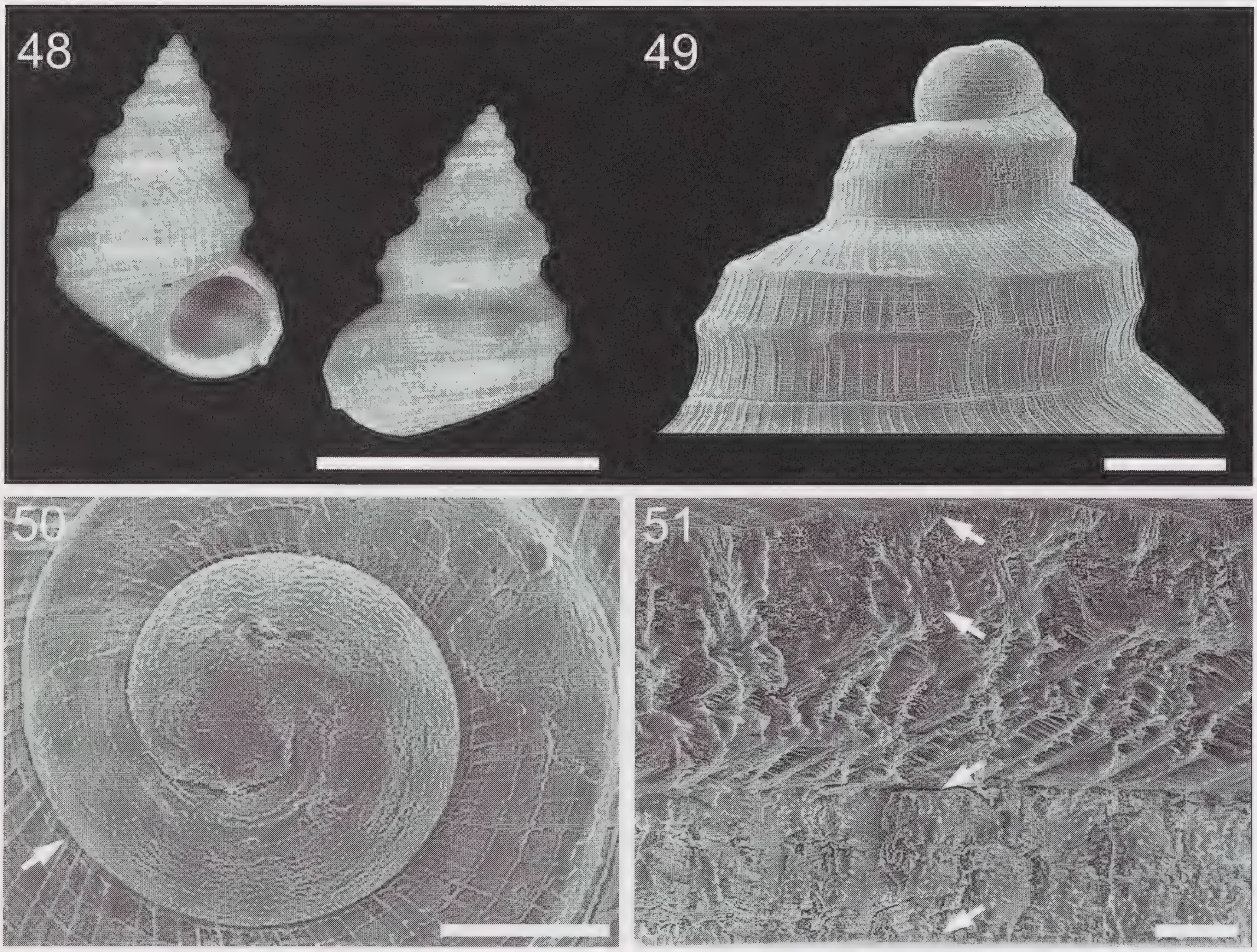

FIGS. 48–51. Shell morphology of *Mysorelloides multisulcata* (IRSNB no. 126). FIG. 48: Adult shell of specimen used in anatomical investigations. Scale bar = 5 mm; FIG. 49: Embryonic shell. Scale bar = 200 µm; FIG. 50: Embryonic shell, apical view. Arrow indicates approximate transition to teleoconch. Scale bar = 100 µm; FIG. 51: Shell microstructure. Cross section through shell parallel to aperture; outside of shell is uppermost. Order of layers from external to internal: (a) irregular, simple prismatic structure, (b) simple radial crossed lamellar structure, (c) simple comarginal crossed lamellar structure, (d) irregular, complex crossed lamellar structure, (e) irregular, simple prismatic structure. Arrows indicate transitions between layers. Scale bar = 20 µm.

rather accurate but not very detailed description of most features. Although Digby (1902) found the anatomy of *Limnotrochus* and *Chytra* to be distinctly similar, she remarked that the affinities of the former were even more difficult to assess. She concluded *Limnotrochus* to be allied to *Chytra* and *Tiphobia*, but likely more near the "stromboid" group (i.e., *Strombus*, *Aporrhais*). Moore (1903) reproduced parts of Digby's (1902) description, and featured an operculum, one row of the radula and the interior of the midgut.

Brown (1994) remarked on the variability in size and number of denticles on radular teeth in comparing the specimen figured by Digby (1902) to one he examined from Kombe, Zambia. West & Cohen (1996) reported three layers of crossed lamellar microstructure in the shell.

Mysorelloides multisulcata (Bourguignat, 1888)

Material Examined: Democratic Republic of Congo: Kalemie (DBL) (4 spms). Tanzania: at Karema, in intestine of the fish *Synodontis melanostictus*, ±30 m (IRSNB no. 123) (4 spms); at Karema (IRSNB no. 126) (8 spms; 2 spms dissected). Zambia: between Butondwe and Kumbula Island, 50 m (DBL) (47 spms).

Shell: Adult shell comprising up to five whorls (Figs. 48, 54). Apical cap of embryonic shell with irregularly, finely textured surface, rapidly giving way to numerous fine spiral threads (Figs. 49, 50, 55). Gradual transition to teleoconch with spiral threads joined by fine axial threads and variable number of prominent,

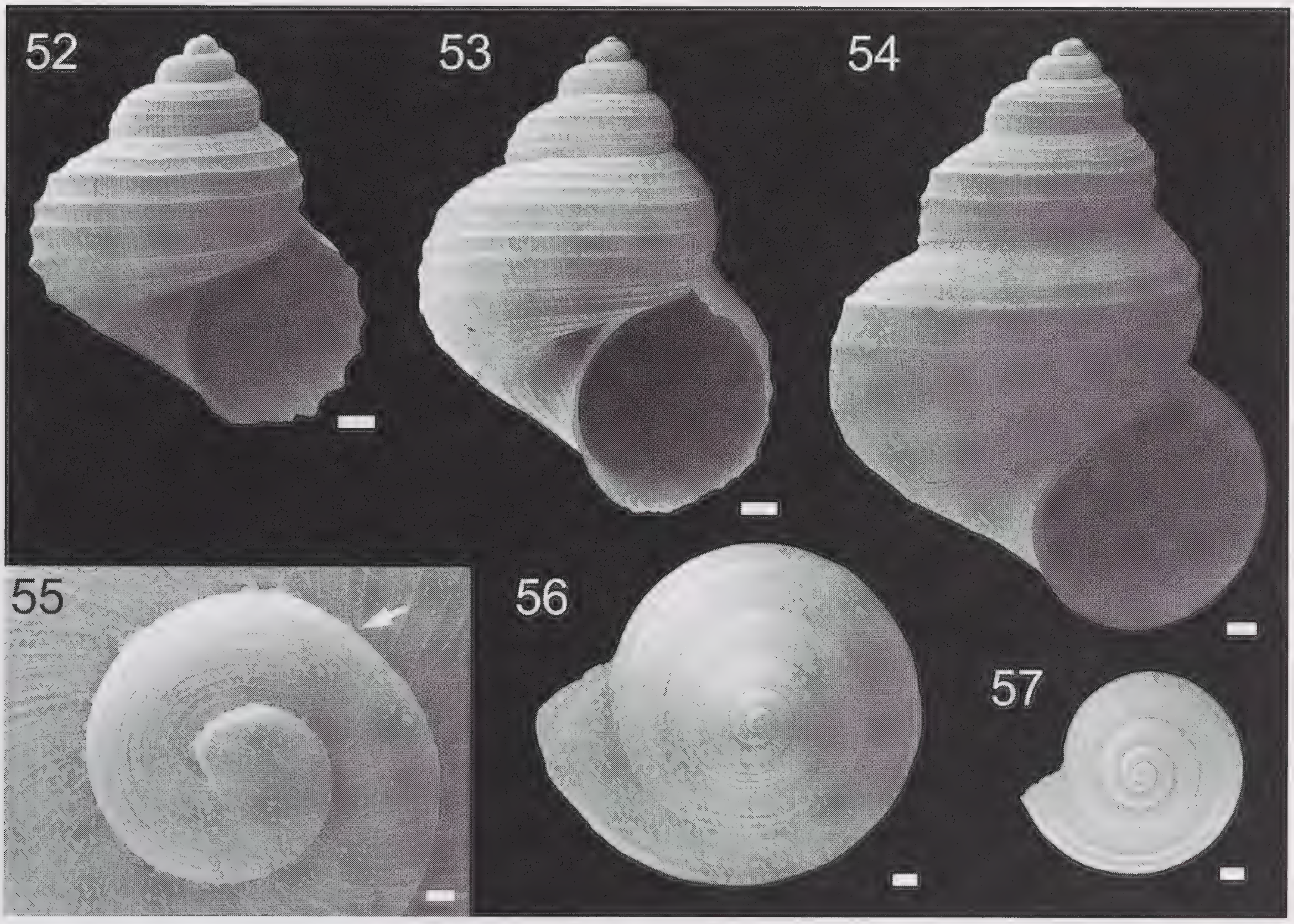

FIGS. 52–57. Shell morphology of *Mysorelloides multisulcata* (DBL). FIG. 52: Juvenile shell. Scale bar = 200 μm; FIG. 53: Juvenile shell. Scale bar = 300 μm; FIG. 54: Shell of sub-adult. Scale bar = 200 μm; FIG. 55: Embryonic shell, apical view. Arrow indicates approximate transition to teleoconch. Scale bar = 20 μm; FIG. 56: Sub-adult, apical view (same specimen as in FIG. 54). Scale bar = 200 μm; FIG. 57: Juvenile, apical view (same specimen as in FIG. 52). Scale bar= 200 μm.

smoothly undulating spiral cords producing reticulate pattern. Spiral threads gradually becoming obsolete over first three teleoconch whorls. Several spiral cords may be more prominent, producing angular whorl profile (Fig. 48), or spiral cords may be more or less equal in prominence and distributed over smoothly rounded whorls (Figs. 52–54). Aperture thickened, holostome. Umbilicus narrow. Shell microstructure (Fig. 51) comprising five layers from external to internal: (1) irregular, simple prismatic structure, (2) simple radial crossed lamellar structure, (3) simple comarginal crossed lamellar structure, (4) irregular, complex crossed lamellar structure, (5) irregular, simple prismatic structure.

External Anatomy: Operculum (Fig. 60) thin, transparent, light amber brown in color. Operculum spiral, comprising approximately 5 whorls, increasing evenly in size.

Foot narrowly ovate, with broad propodium bearing shallow pedal gland along anterior margin (Fig. 59: ap). Columellar muscle extending to base of mantle cavity. In females, ovipositor (Fig. 59: ovp) present on right side of foot, below eye, just behind foot sole margin at junction between propodium and mesopodium. Aperture of ovipositor forming simple, oblique slit bounded by tall folds; lumen shallow, u-shaped with prominent fold projecting from floor. Finely grooved tract to foot sole and ciliated egg groove between ovipositor and pallial oviduct lacking.

Retracted cephalic tentacles (Fig. 61: t) rather smooth, long, tapering, slightly longer than snout. Eyes located on small protuberances at base of tentacles. Snout (Fig. 61: sn) broad, squarish, with small mouth opening ventrally at tip.

Mantle cavity short, extending approximately one half whorl. Hypobranchial gland weakly developed (Fig. 58: hg). Mantle edge smooth. Ctenidium (Figs. 58, 59, 61: ct) extending from near mantle margin to rear of mantle cavity; leaflets narrowly triangular.

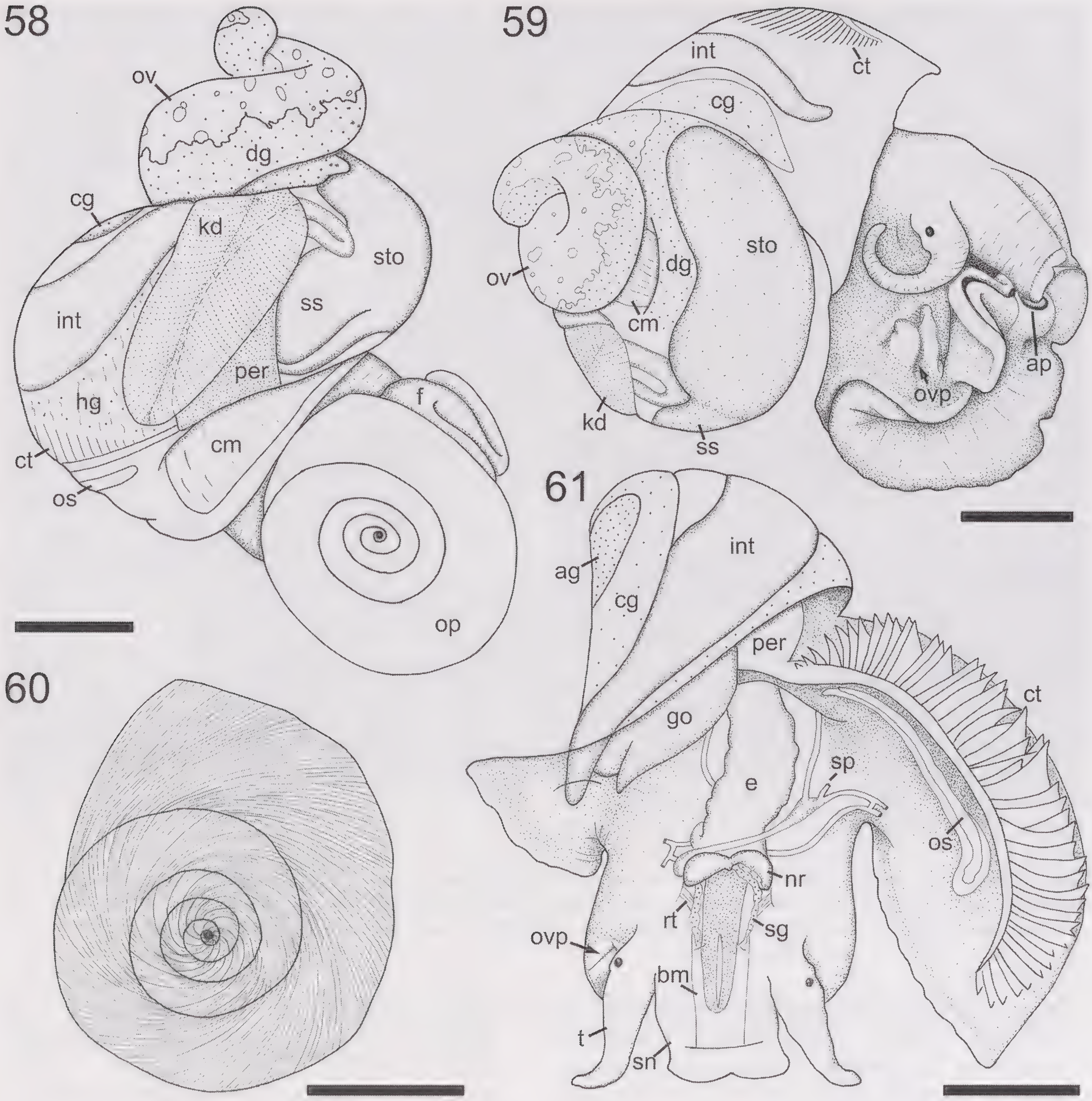

FIGS. 58–61. External anatomy of *Mysorelloides multisulcata* (IRSNB no. 126). FIG. 58: External view of organs in visceral mass. Dashed line indicates extent of pericardium under main kidney chamber; FIG. 59: External view of organs in visceral mass; right lateral view of female head-foot with ovipositor; FIG. 60: Operculum; FIG. 61: Dorsal view of mantle cavity and organs of cephalic hemocoel seen by transparency. Anterior is below. Abbreviations: ag, albumen gland; ap, anterior pedal gland; bm, buccal mass; capsule gland; cm, columellar muscle; ct, ctenidium; dg, digestive gland; e, esophagus; go, pallial gonoduct; hg, hypobranchial gland; int, intestine; kd, kidney; nr, circumesophageal nerve ring; op, operculum; os, osphradium; ov, ovary; ovp, ovipositor; per, pericardium; rt, buccal retractor; sg, salivary gland; sn, snout; sp, supraesophageal ganglion; ss, style sac; sto, stomach; t cephalic tentacle. Scale bars = 1 mm.

Osphradium (Figs. 58, 61: os) smooth, long, roughly two thirds of ctenidium in length, in shallow depression.

Alimentary System: Foregut. Radula taenioglossate (Fig. 62). Rachidian (Fig. 63) rectangular, wider than tall, with lower margin tapering to narrow, squarish projection. Upper margin convex to slightly concave, with cutting edge bearing single, prominent, pointed central cusp bounded by six to 14 fine, pointed denticles on each side (Fig. 64); denticles often fused to each other and to central cusp. Lateral teeth with very long

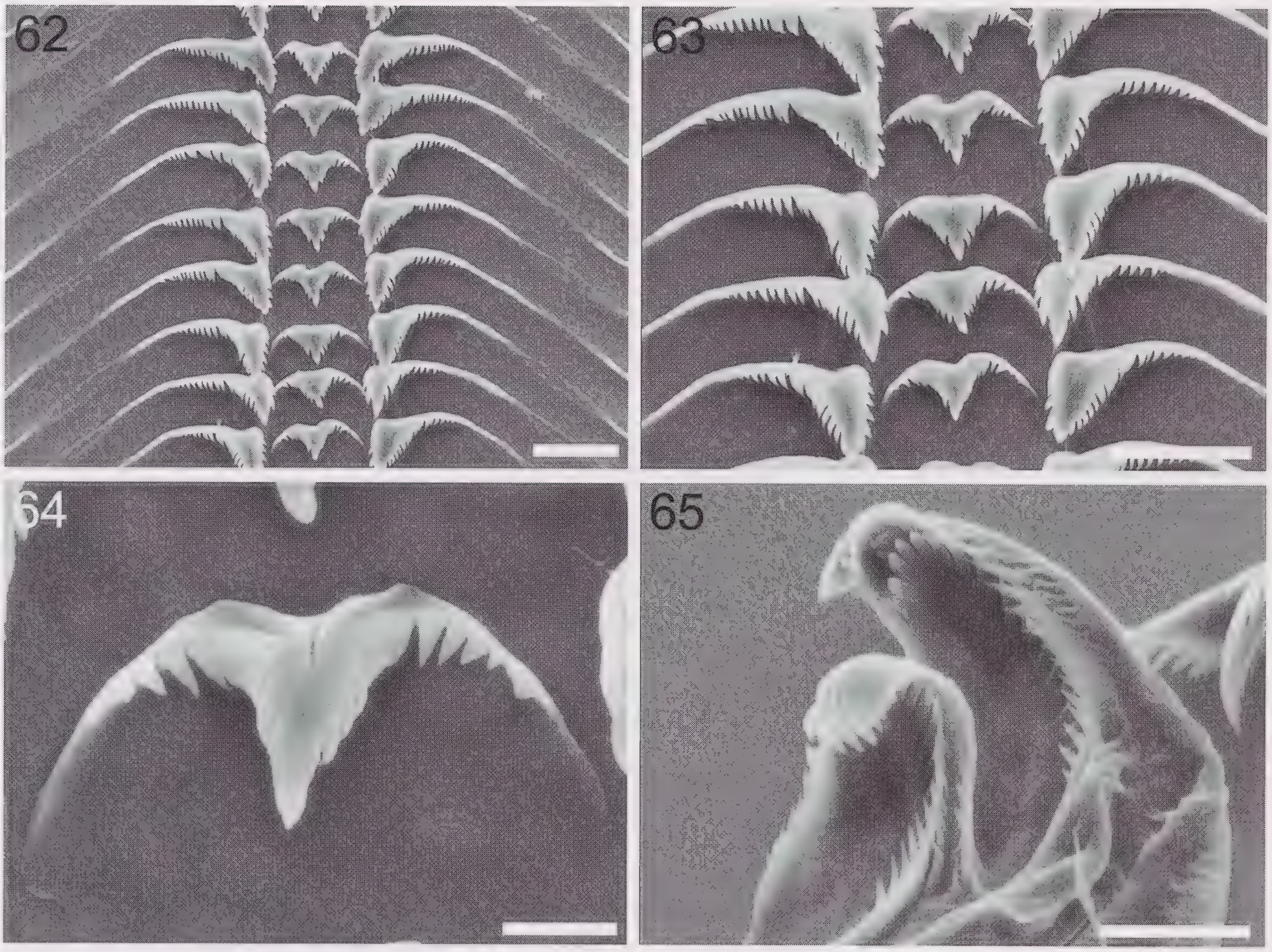

FIGS. 62-65. Radula morphology of *Mysorelloides multisulcata* (IRSNB no. 126). FIG. 62: Rachidian and lateral teeth. Scale bar = 20 µm; FIG. 63: Rachidian and lateral teeth. Scale bar = 20 µm; FIG. 64: Rachidian. Scale bar = 5 µm; FIG. 65: Marginal teeth. Scale bar = 10 µm.

lateral extensions (Fig. 62), roughly twice as long as cutting edge. Cutting edge triangular with five to seven inner and 17–23 outer pointed denticles. Marginal teeth (Fig. 65) long, slender, with narrow, elongate, rounded tips bearing numerous fine, pointed denticles; inner marginal with ~20–25 denticles around tip and along inner edge only, outer marginal with ~30–35 denticles along distal one third of inner and outer edges. Number of denticles on all teeth variable between individuals.

Mouth opening ventrally at anterior end of snout. Buccal mass (Fig. 61: bm) narrow, elongate; small odontophore occupying posterior half of buccal cavity. Narrowly triangular, glandular subradular organ extending along floor of buccal cavity at anterior end of odontophore. Small, paired jaw dorsally flanking mouth at anterior ends of dorsal folds. Shallow, nonglandular buccal pouches extending underneath dorsal folds adjacent to buccal ganglia at rear of buccal cavity. Salivary glands (Fig. 61: sg) forming short, coiled, unbranched tubules, opening dorsolaterally alongside odontophore. Salivary glands asymmetrical with left gland overlying circumesophageal nerve ring (Fig. 61: nr), and right gland terminating within nerve ring. Thick buccal retractors (Fig. 61: rt) extending from rear wall of buccal mass, inserting on lateral walls of cephalic hemocoel immediately anterior to nerve ring. Nerve ring lying short distance back from posterior end of cephalic tentacles. Radular sac short, projecting slightly past end of buccal mass and curving dorsally underneath anterior esophagus. Within anterior esophagus, short, glandular midventral fold just behind odontophore. Paired ventral longitudinal folds commencing immediately behind midventral fold. Walls of anterior and midesophagus with paired, longitudinal ventral and dorsal folds and numerous additional, longitudinal folds of roughly equal prominence; dorsal and ventral folds fusing with each other (i.e., right dorsal fold with right ventral fold) at posterior

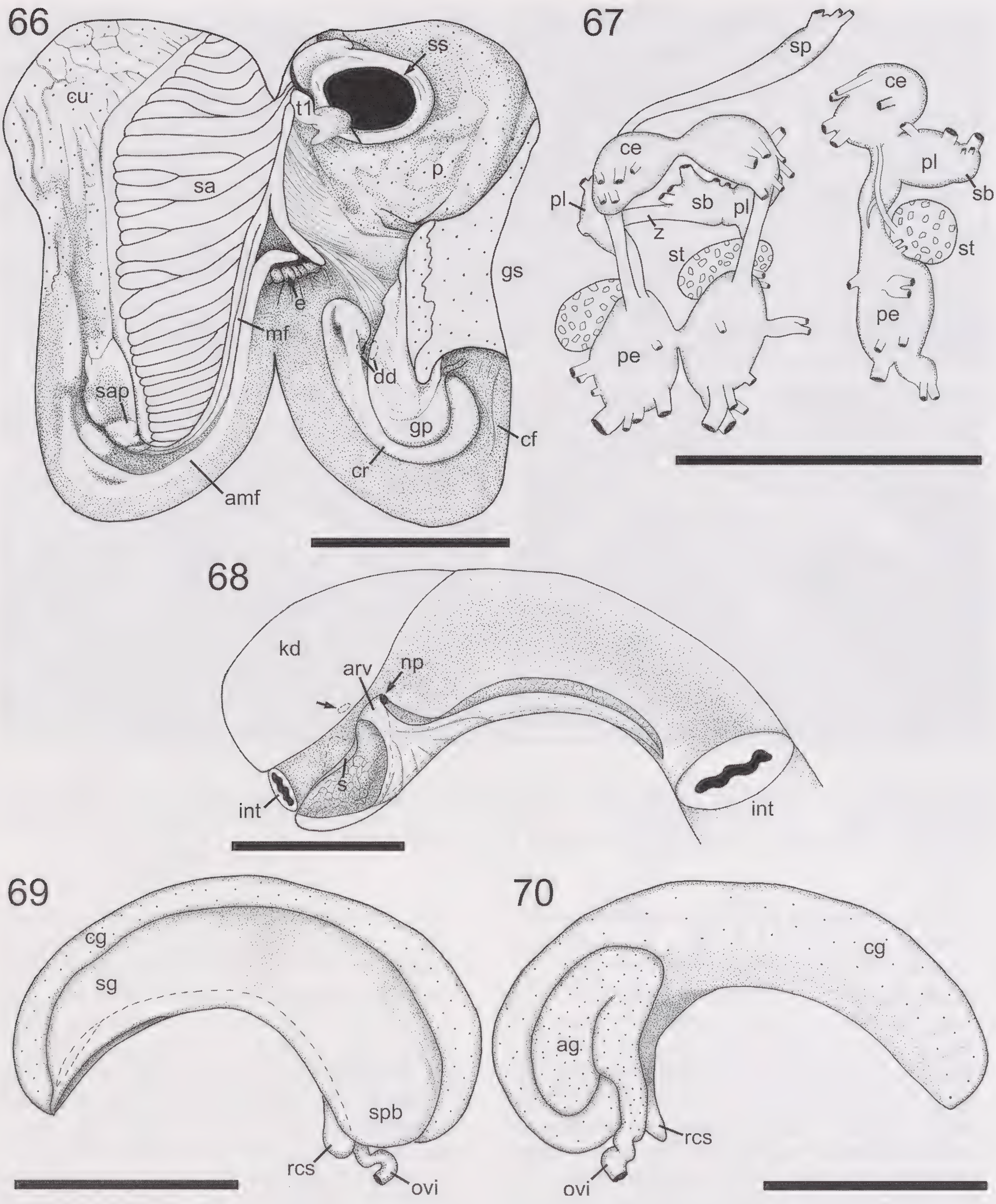

FIGS. 66–70. Internal anatomy of *Mysorelloides multisulcata* (IRSNB no. 126). FIG. 66: Midgut anatomy. Dorsal view, anterior is uppermost; FIG. 67: Circumesophageal nerve ring. Frontal view (left) and left lateral view (right); FIG. 68: Kidney anatomy. Internal view of bladder. Lateral view, anterior is at right. Roof of bladder (below intestine) cut open to reveal interior; FIG. 69: External, left lateral view of pallial oviduct. Anterior is at left; FIG. 70: External, right lateral view of pallial oviduct. Anterior is at right. Abbreviations: ag, albumen gland; amf, accessory marginal fold; arv, afferent renal vessel; ce, cerebral ganglion; cf, caecal fold; cg, capsule gland; cr, crescentic ridge; cu, cuticularized region in midgut roof; dd, digestive gland duct; e, esophagus; gp, glandular pad; gs, gastric shield; int, intestine; kd, kidney; mf, marginal fold; np, nephropore; ovi, renal oviduct; p, crystalline style pocket; pe, pedal ganglion; pl, pleural ganglion; rcs, seminal receptacle; sa, sorting area; sb, subesophageal ganglion; sap, sorting area pad; sg, seminal groove; sp, supraesophageal ganglion; spb, spermatophore bursa; ss, style sac; st, statocyst; t1, major typhlosole; z, zygoneury. Scale bars = 1 mm.

end of midesophagus, enclosing shallow, smooth, rear-projecting triangular troughs. Midesophageal gland lacking.

Midgut. Esophagus opening to gastric chamber floor at left (Fig. 66: e). Marginal fold (Fig. 66: mf) extending anteriorly alongside major typhlosole (Fig. 66: t1), then turning posteriorly bordering edge of sorting area (Fig. 66: sa). Sorting area rectangular, with rounded posterior margin. Marginal fold elaborated into small pad at left, posterior tip of sorting area (Fig. 66: sap). Accessory marginal fold (Fig. 66: amf) emerging from left side of esophageal aperture, paralleling marginal fold, curving anteriorly around posterior end of sorting area; accessory marginal fold bifurcate posteriorly. Epithelium of midgut floor finely, regularly grooved at right of marginal fold and along projecting tip of major typhlosole. Anterior midgut roof at left of sorting area deeply, irregularly creased, cuticularized (Fig. 66: cu). Gastric shield (Fig. 66: gs) moderately large, continuous with cuticle of midgut roof and crystalline style pocket (Fig. 66: p). Creased, weakly developed fold bounding grooved u-shaped depression below lip of style sac (Fig. 66: ss) in one of two specimens examined. Glandular pad (Fig. 66: gp) small, broadly rounded; accessory pad at anterior end lacking. Crescentic ridge (Fig. 66: cr) extending back from near esophageal aperture and fusing to right side of glandular pad, bounding deep, narrow crescentic groove. Proximal tip of crescentic ridge bounding deep pouch with two digestive gland ducts. Caecum lacking. Single, weakly developed longitudinal fold (Fig. 66: cf) behind gastric shield, opposite glandular pad. Style sac (Fig. 58: ss) communicating proximally with intestine. Crystalline style present.

Hindgut. Proximal intestine (Fig. 58: int) passing below distal tip of style sac, then extending posteriorly alongside style sac (Fig. 58: ss), forming small loop across right side proximal style sac adjacent to main gastric chamber (Fig. 58: sto). Intestine continuing forward, passing under posterior end of main kidney chamber (Fig. 58: kd), entering pallial roof between bladder and main kidney chamber, to papillate anus near mantle margin (Fig. 61: int).

Reno-Pericardial System: Voluminous kidney (Fig. 58: kd) extending from near anterior end of main gastric chamber (Fig. 58: sto) alongside style sac and pericardium into mantle roof. Kidney lumen partially subdivided into two main chambers. Main chamber (Figs. 58, 68: kd) extending full length of kidney, surrounding pericardium dorsally and at right, anteriorly overhanging base of mantle cavity; lumen mostly occluded by excretory tubules developed in roof and along walls. Small bladder at right of main chamber, extending into pallial roof between intestine (Fig. 58: int) and pallial gonoduct (Fig. 58: cg). Bladder (exposed chamber in Fig. 68) communicating with main chamber via small aperture (Fig. 68: arrow) just behind afferent renal vessel (Fig. 68: arv). Bladder partially subdivided posteriorly by incomplete horizontal septum of excretory tissue (Fig. 68: s), separating shallow, narrow chamber above. Large sheet of excretory tubules branching from afferent renal vessel and extending anteriorly along bladder floor, partially separating narrow, shallow ventral chamber below. Nephridial gland absent.

Narrow, deep pericardium (Fig. 58: per) extending underneath kidney alongside style sac (Fig. 58: ss) past intestinal loop.

Nervous System: Cerebral ganglia (Fig. 67: ce) connected by short, stout commissure, each ganglion producing six nerves (optic, statocyst, tentacular, and three labial nerves). Buccal ganglia lying ventrolaterally at base of buccal mass, at inner edge of retractor muscles, below anterior esophagus. Pleural ganglia (Fig. 67: pl) lying behind and below cerebral ganglia connected to cerebral ganglia by short, thick connectives. Pedal ganglia (Fig. 67: pe) with two prominent anterior nerves and approximately five to seven smaller accessory nerves. Statocysts (Fig. 67: st) with numerous angular statoconia present dorsally alongside pedal ganglia behind pedal connectives. Subesophageal ganglion (Fig. 67: sb) separated from left pleural ganglion by slight constriction. In addition to connectives to left pleural and visceral ganglia, subesophageal ganglion producing two stout nerves, two fine nerves and zygoneurous connection to right pleural ganglion (Fig. 67: z). Long connective uniting right pleural and supraesophageal ganglia (Fig. 67: sp), the latter lying at left of midesophagus (see Fig. 61: sp). Dialyneury formed between pallial nerve of left pleural ganglion and osphradial nerve of supraesophageal ganglion at junction of mantle roof and floor. Single visceral ganglion present at base of cephalic hemocoel.

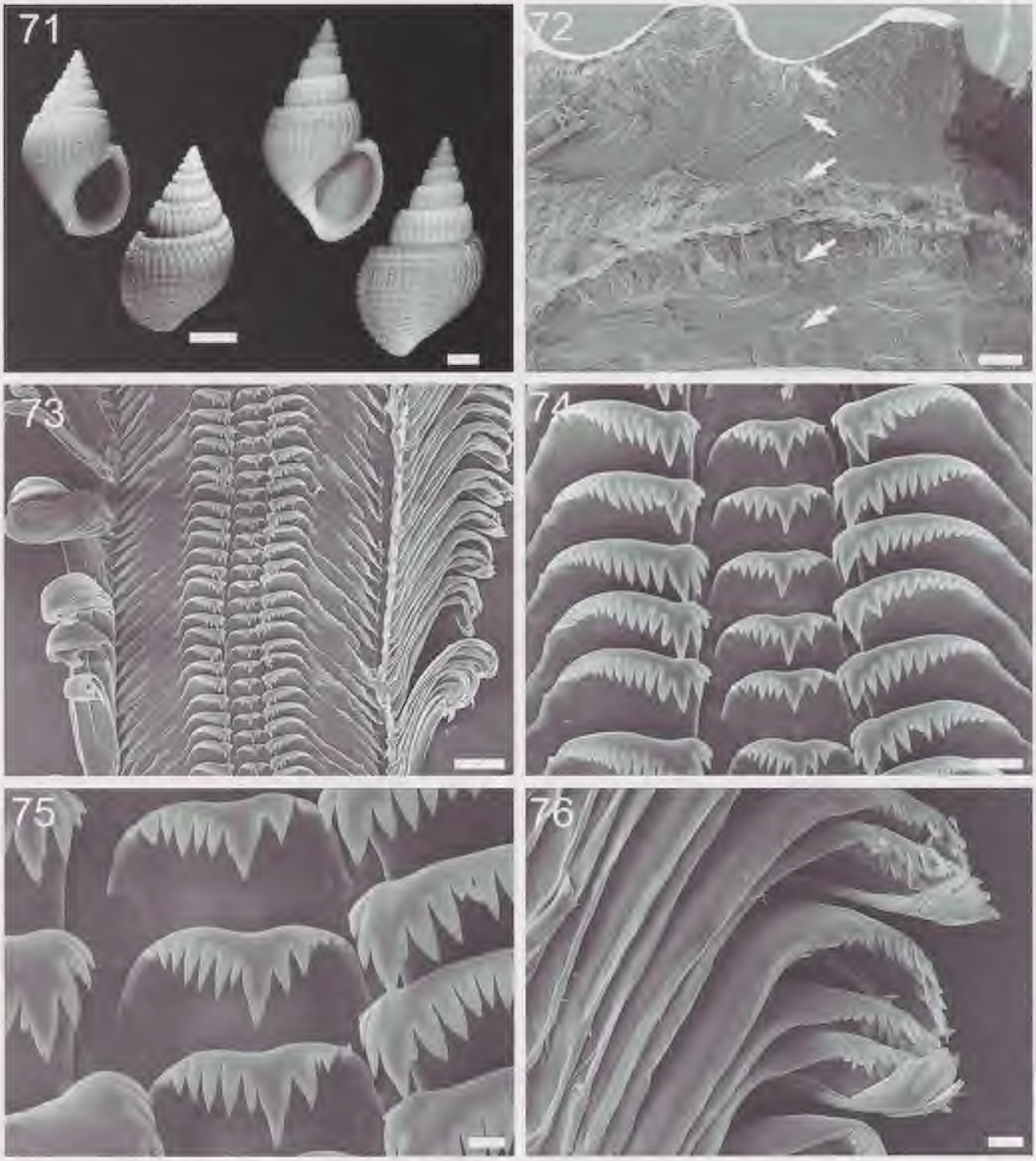

FIGS. 71–76. Shell and radula morphology of *Paramelania iridescens* (ZMB 220.037, except when noted). FIG. 71: Adult shell. At left, shell of specimen used in anatomical investigations; at right, more mature specimen (USNM 857897). Scale bar = 5 mm; FIG. 72: Shell microstructure. Cross section through shell parallel to aperture; outside of shell is uppermost. Order of layers from external to internal: (a) irregular, simple prismatic structure, (b) simple radial crossed lamellar structure, (c) simple comarginal crossed lamellar structure, (d) simple radial crossed lamellar structure, (e) irregular, complex crossed lamellar structure, f) irregular, simple prismatic structure. Arrows indicate transitions between layers. Scale bar = 100 µm; FIG. 73: Radula. Scale bar = 40 µm; FIG. 74: Rachidian and lateral teeth. Scale bar = 10 µm; FIG. 75: Rachidian. Scale bar = 2 µm; FIG. 76: Marginal teeth. Scale bar = 6 µm.

Female Reproductive System: Gonad (Figs. 58, 59: ov) dorsally overlying digestive gland (Fig. 59: dg) from tip of visceral mass to posterior end of gastric chamber (Fig. 59: sto). Oviduct emerging ventrally from ovary. Renal oviduct (Figs. 69, 70: ovi) forming short recurvent loop behind mantle cavity before entering base of glandular oviduct. Pallial oviduct, with proximal albumen (Fig. 70: ag) and distal capsule glands (Figs. 69, 70: cg). Albumen gland forming rear-facing c-shaped tube at posterior end of pallial oviduct; capsule gland developed along dorsal crest of pallial oviduct. Glandular tissue of capsule and albumen glands with opposing flattened surfaces bounding morphologically dorsal gonoductal groove. Narrow vagina along anterior one third of oviduct opening to sperm gutter (Fig. 69: sg) in median lamina. Gutter leading posteriorly to elongate, broad spermatophore bursa (Fig. 69: spb). Inner wall of median lamina fusing to outer wall, restricting communication between spermatophore bursa and ventral channel to short, anterior slit (Fig. 69: double dashed line). Ventral edge of median lamina inner wall (Fig. 69: single dashed line) continuing posteriorly as shallow groove above ventral channel, posteriorly enclosing entrance to seminal receptacle (Figs. 69, 70: rcs). Communication between sperm gutter and ventral channel bounded by two folds: one shallow dorsal fold along outer ventral edge of median lamina inner wall, and one prominent ventral fold extending along ventral edge of vagina. Dorsal and ventral fold fusing posteriorly, continuing as single, prominent longitudinal fold along length of bursa floor with central longitudinal gutter continuous with communication to ventral channel.

Male Reproductive System: Male reproductive anatomy unknown.

Remarks: Leloup (1953) reported the operculum to be spiral, a rachidian broader than tall with 9–11/1/9–11; lateral teeth with 3–4/1/~20; marginal teeth with ~20/~15. Riedel (1993) provided a description of the embryonic shell, including SEM micrographs, of *M. multisulcata* specimens misidentified as *Limnotrochus thomsoni* (fig. 21; pl. 4, figs. 5, 6).

Paramelania iridescens
(Moore, 1898)

Material Examined: (DBL) (1 spm); (USNM 250717) (1 spm); (ZMB 52.540) (1 spm); (ZMB 53.548) (1 spm); (ZMB 55.030) (1 spm); (ZMB 85.792) (1 spm); (ZMB 92.364) (2 spms); (CM 62.29277) (3 spms); (CM 62.29435) (3 spms); (NHMB 10.846a) (1 spm). Burundi: Nyanza-Lac, 2 km SW Military Point, 20 m (04°21'S, 29°36'E) (USNM 882019) (5 spms); Bujumbura (ZMB 220.053) (2 spms); same (ZMB 220.163) (3 spms); same (ZMB 220.164) (2 spms). Tanzania: Kigoma (ZMB 85.792) (1 spm); same (ZMB 220.120) (29 spms); same (ZMB 220.037) (4 spms; 3 spms dissected); between Kigoma & Ujiji, 35–60 m (ZMB 220.173) (2 spms); Viapili, 100–120 ft (07°27'S, 30°37'E) (USNM 857897) (2 spms). Zambia: Chipata Bay, 80 m (08°41.700'S, 31°08.952'E) (ZMB 220.099) (1 spm dissected); Mpulungu, 30 m (DBL) (5 spms).

Shell: Adult shell comprising up to nine whorls, typically with broken apex (Fig. 71). Embryonic shell unknown. Early teleoconch whorls rapidly developing roughly five to six spiral threads and closely packed fine axial threads producing reticulate appearance. By third teleoconch whorl, opisthocyrt axial ribs appearing, producing nodes at intersection with axial threads. Nodes on uppermost spiral thread gradually becoming more prominent, and thread may be slightly separated from remaining, regularly spaced threads. Uppermost thread also slightly separated from suture, producing flattened shoulder. Number of spiral threads above suture rather constant through ontogeny. Whorl profile on early teleoconch whorls may be rounded or more angular in specimens with early development of flattened shoulder; later whorls gradually becoming more flattened. Aperture thickened, slightly flaring, with weakly developed anterior and posterior siphon. Single spine may be developed on shoulder above posterior siphon in adults. Umbilicus lacking. Shell microstructure (Fig. 72) comprising six layers from external to internal: (1) irregular, simple prismatic structure, (2) simple radial crossed lamellar structure, (3) simple comarginal crossed lamellar structure, (4) simple radial crossed lamellar structure, (5) irregular, complex crossed lamellar structure, (6) irregular, simple prismatic structure.

External Anatomy: Operculum (Fig. 78) thick, concave, dark brown in color. Operculum concentric with central, paucispiral nucleus; nucleus comprising approximately three whorls.

Foot broadly ovate, with broad propodium bearing shallow pedal gland (Fig. 77: ap) along anterior margin. In females, ovipositor present on right side of foot, below eye, just behind foot sole margin. Aperture of ovipositor forming simple, oblique slit on slight rise. Finely grooved tract to foot sole and ciliated

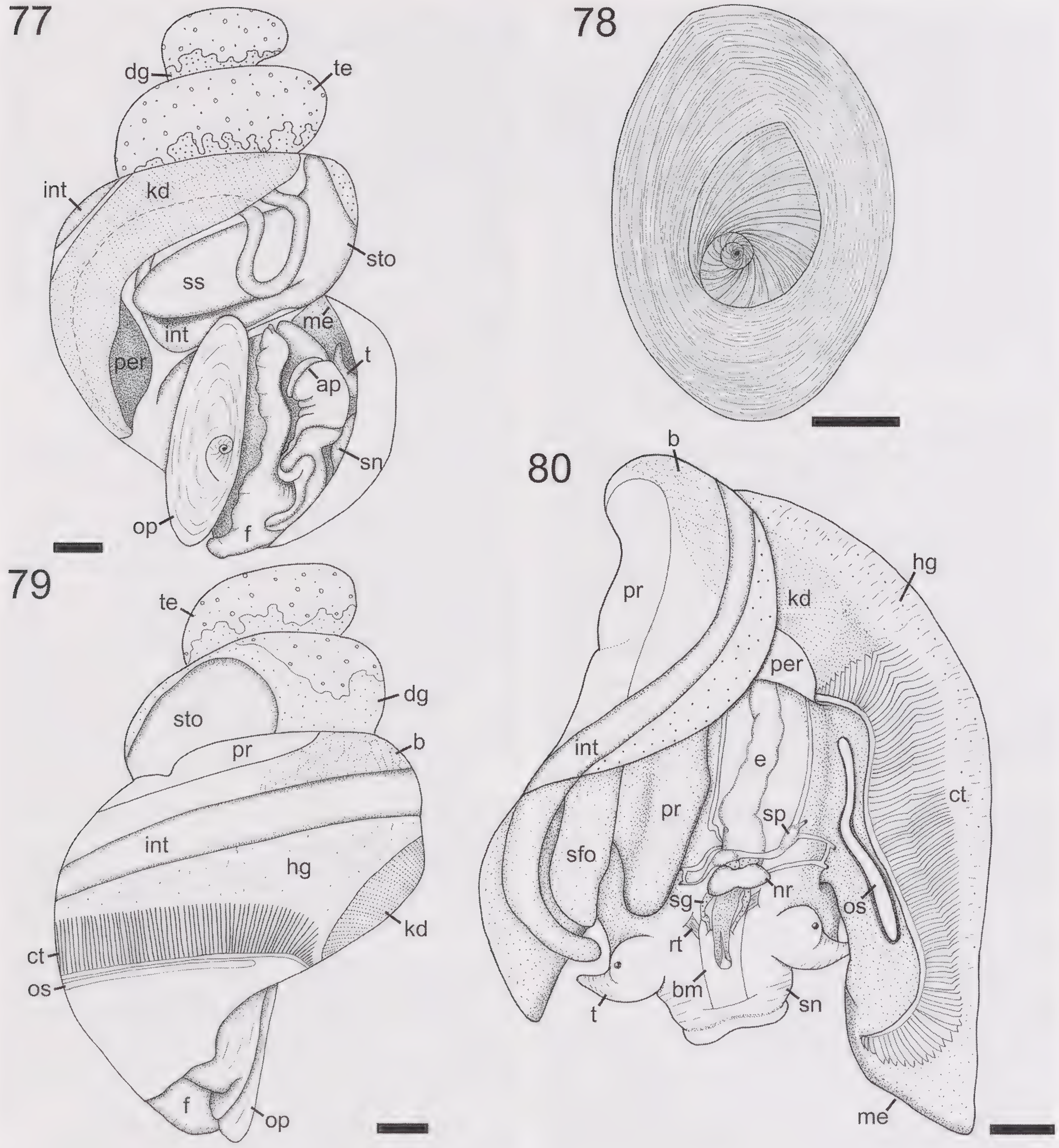

FIGS. 77–80. External anatomy of *Paramelania iridescens* (ZMB 220.037). FIG. 77: External view of organs in visceral mass. Dashed line indicates extent of pericardium under main kidney chamber; FIG. 78: Operculum; FIG. 79: External view of organs in visceral mass; FIG. 80: Dorsal view of mantle cavity and organs of cephalic hemocoel seen by transparency. Anterior is below. Abbreviations: ap, anterior pedal gland; b, bladder; bm, buccal mass; cm, columellar muscle; ct, ctenidium; dg, digestive gland; e, esophagus; f, foot; hg, hypobranchial gland; int, intestine; kd, kidney; me, mantle edge; nr, circumesophageal nerve ring; op, operculum; os, osphradium; per, pericardium; pr, prostate; rt, buccal retractor; sfo, spermatophore forming organ; sg, salivary gland; sn, snout; sp, supraesophageal ganglion; ss, style sac; sto, stomach; t cephalic tentacle; te, testis. Scale bars = 1 mm.

egg groove between ovipositor and pallial oviduct lacking.

Retracted cephalic tentacles (Figs. 77, 80: t) smooth, short, triangular, slightly shorter than snout in length. Eyes located on small protuberances at base of tentacles. Snout (Figs. 77, 80: sn) broad, squarish, with small mouth opening ventrally at tip.

Mantle cavity short, extending approximately one half whorl. Hypobranchial gland moderately well developed (Figs. 79, 80: hg), with transverse grooves. Mantle edge smooth (Fig. 80: me). Ctenidium (Figs. 79, 80: ct) extending from near mantle margin to rear of mantle cavity; leaflets broadly triangular with narrow, projecting apices. Osphradium (Figs. 79, 80: os) smooth, long, narrow, slightly less than half of ctenidium in length, in shallow depression.

Alimentary System: Foregut. Radula taenioglossate (Fig. 73). Rachidian (Fig. 74) rectangular, wider than tall, with lower margin tapering to narrow, v-shaped projection. Upper margin slightly concave, with cutting edge with single, prominent, pointed central cusp bounded by two to seven fine, pointed denticles on each side (Fig. 75). Lateral teeth with extremely long lateral extensions (Fig. 73), roughly 2.5 length of cutting edge. Cutting edge with single, prominent pointed cusp flanked by two to four inner and 10–12 outer pointed denticles. Marginal teeth (Figs. 73, 76) long, slender, with narrow, elongate, rounded tips bearing ~13–16 fine, rounded denticles of similar size and shape around tip and along distal one fourth of inner edge. Number of denticles on all teeth variable between individuals.

Mouth opening ventrally at anterior end of snout. Buccal mass (Fig. 80: bm) narrow, elongate; small odontophore occupying posterior half of buccal cavity. Narrowly triangular, glandular subradular organ extending along floor of buccal cavity at anterior end of odontophore. Small, paired jaw dorsally flanking mouth at anterior ends of dorsal folds. Shallow, nonglandular buccal pouches extending underneath dorsal folds adjacent to buccal ganglia at rear of buccal cavity. Salivary glands (Fig. 80: sg) forming short, slightly undulating simple tubules, opening dorsolaterally alongside odontophore; salivary glands just passing through circumesophageal nerve ring (Fig. 80: nr) but not extending posteriorly. Thick buccal retractors (Fig. 80: rt) extending from rear wall of buccal mass, inserting on lateral walls of cephalic hemocoel anterior to nerve ring. Nerve ring lying short distance back from posterior end of cephalic tentacles. Radular sac short, projecting slightly past end of buccal mass and curving dorsally underneath anterior esophagus. Within anterior esophagus, tall, glandular midventral fold just behind odontophore. Paired ventral longitudinal folds commencing immediately behind midventral fold. Walls of anterior and midesophagus with paired, longitudinal ventral and dorsal folds; dorsal and ventral folds continuing through midesophagus and continuous with folds in posterior esophagus. Posterior esophagus with numerous folds of equal height. Midesophageal gland lacking.

Midgut. Best available specimen not well preserved. Esophagus opening to gastric chamber floor at left (Fig. 81: e). Marginal fold (Fig. 81: mf) extending anteriorly alongside major typhlosole (Fig. 81: t1), then turning posteriorly bordering edge of sorting area (Fig. 81: sa). Sorting area rectangular, with rounded posterior margin. Marginal fold elaborated into small, elongate pad at left, posterior tip of sorting area (Fig. 81: sap). Accessory marginal fold (Fig. 81: amf) obsolete anteriorly, curving anteriorly around posterior end of sorting area, bifurcate posteriorly. Midgut roof at left of sorting area cuticularized (Fig. 81: cu). Gastric shield (Fig. 81: gs) large, continuous with cuticle of midgut roof and crystalline style pocket (Fig. 81: p). Thin, weakly developed fold bounding u-shaped depression (Fig. 81: u) below lip of style sac (Fig. 81: ss). Glandular pad (Fig. 81: gp) large, elongate, broadly rounded; accessory pad present at left, anterior tip (Fig. 81: ap). Crescentic ridge (Fig. 81: cr) extending back from near esophageal aperture and fusing to right side of glandular pad, bounding shallow crescentic groove. Proximal crescentic ridge bounding deep pouch with two digestive gland ducts (Fig. 81: dd). Shallow, elongate caecum (Fig. 81: c) extending ventrally under glandular pad behind gastric shield. Single, weakly developed longitudinal fold (Fig. 81: cf) behind gastric shield, opposite caecum. Style sac (Fig. 77: ss) communicating proximally with intestine (Fig. 77: int). Crystalline style present.

Hindgut. Proximal intestine (Fig. 77: int) passing below distal tip of style sac, then extending posteriorly alongside style sac (Fig. 77: ss), forming broad loop over proximal style sac adjacent to main gastric chamber (Fig. 77: sto). Intestine continuing forward, passing under posterior end of main kidney chamber (Fig. 77: kd), entering pallial roof between bladder (Figs. 79, 80: b) and main kidney chamber, to papillate anus near mantle margin (Fig. 80: int).

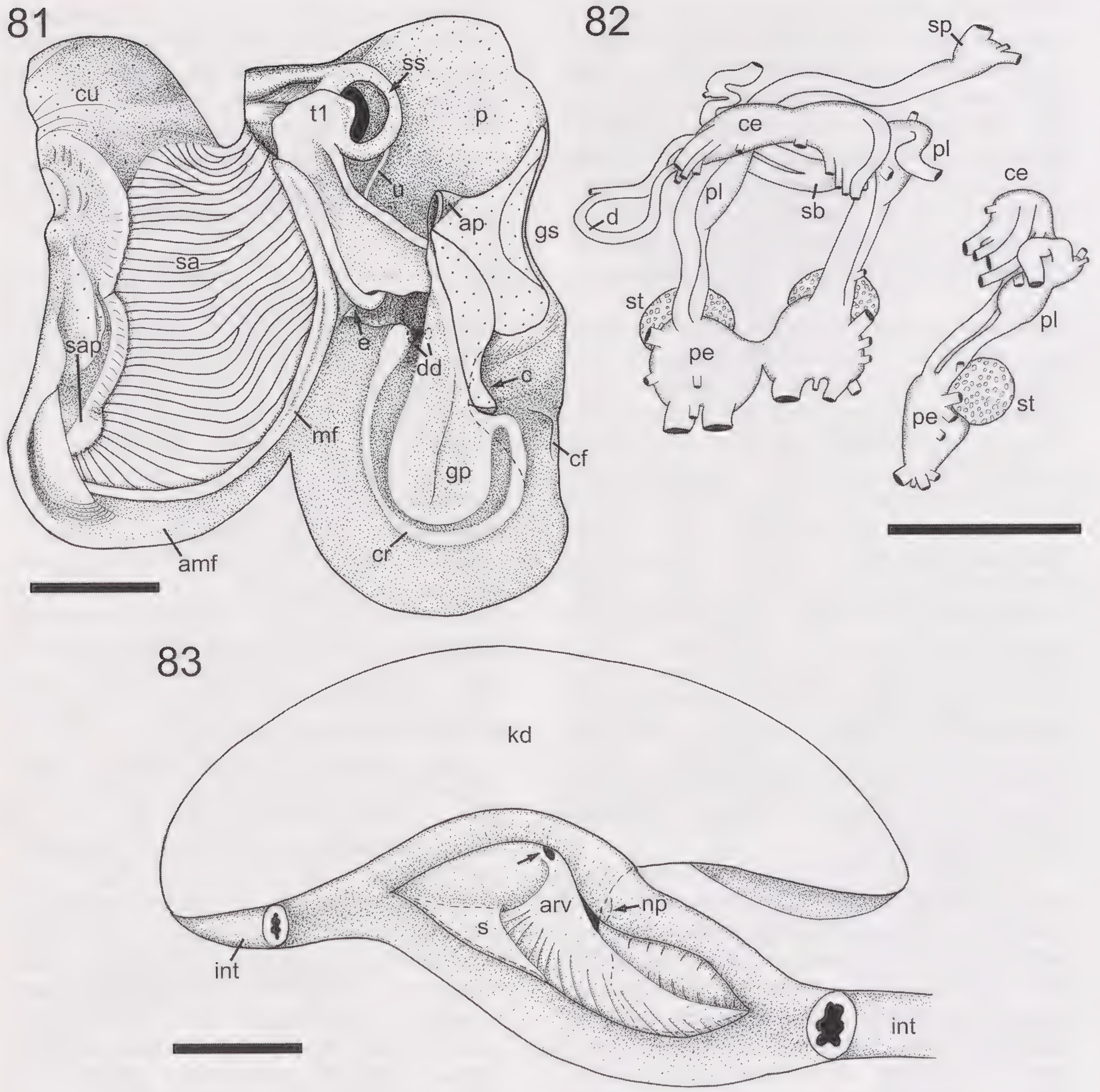

FIGS. 81–83. Internal anatomy of *Paramelania iridescens* (ZMB 220.037). FIG. 81: Midgut anatomy. Dorsal view, anterior is uppermost; FIG. 82: Circumesophageal nerve ring. Frontal view (left) and left lateral view (right); FIG. 83: Kidney anatomy. Internal view of bladder. Lateral view, anterior is at right. Roof of bladder (below intestine) cut open to reveal interior. Abbreviations: amf, accessory marginal fold; ap, accessory pad; arv, afferent renal vessel; c, caecum; ce, cerebral ganglion; cf, caecal fold; cr, crescentic ridge; cu, cuticularized region in midgut roof; d, dialyneury; dd, digestive gland duct; e, esophagus; gp, glandular pad; gs, gastric shield; int, intestine; kd, kidney; mf, marginal fold; np, nephropore; p, crystalline style pocket; pe, pedal ganglion; pl, pleural ganglion; s, septum; sa, sorting area; sb, subesophageal ganglion; sap, sorting area pad; sp, supraesophageal ganglion; ss, style sac; st, statocyst; t1, major typhlosole; u, u-shaped fold. Scale bars = 1 mm.

Reno-Pericardial System: Voluminous kidney (Fig. 77: kd) extending from anterior end of main gastric chamber (Fig. 77: sto) alongside style sac and pericardium into mantle roof. Kidney lumen partially subdivided into two main chambers. Main chamber (Figs. 77, 83: kd) extending full length of kidney, surrounding pericardium dorsally and at right, anteriorly overhanging base of mantle cavity; lumen mostly occluded by excretory tubules developed in roof and along walls. Large bladder (Figs. 79, 80: b) at right of main chamber, extending into pallial roof between intestine (Fig. 79: int) and pallial gonoduct (Fig. 79: pr). Bladder (exposed chamber in Fig. 83) communicating with main chamber via small aperture (Fig. 83: arrow) just behind afferent renal vessel (Fig. 83: arv). Bladder partially subdivided posteriorly by incomplete horizontal septum of excretory tissue (Fig. 83: s). Large sheet of excretory tubules branching from afferent renal vessel and extending anteriorly along bladder floor, partially separating shallow ventral chamber below. Nephridial gland absent.

Narrow, deep pericardium (Fig. 77: per) extending underneath kidney alongside style sac (Fig. 77: ss) to intestinal loop.

Nervous System: Cerebral ganglia (Fig. 82: ce) separated by slight constriction, each ganglion producing six to seven nerves (optic, statocyst, tentacular, and three to four labial nerves). Buccal ganglia lying ventrolaterally at base of buccal mass, adjacent to retractor muscles, at outer edges of anterior esophagus. Pleural ganglia (Fig. 82: pl) lying behind and below cerebral ganglia connected to cerebral ganglia by short, thick connectives. Pedal ganglia (Fig. 82: pe) with two prominent anterior nerves and approximately four to five smaller accessory nerves. Statocysts (Fig. 82: st) with numerous angular statoconia present dorsally alongside pedal ganglia behind pedal connectives. Subesophageal ganglion (Fig. 82: sb) separated from left pleural ganglion by slight constriction. In addition to connectives to left pleural and visceral ganglia, subesophageal ganglion producing two stout nerves, one of which forming dialyneurous connection with pallial nerve from right pleural ganglion (Fig. 82: d). Long connective uniting right pleural and supraesophageal ganglia (Fig. 82: sp), the latter lying at left of midesophagus (Fig. 80: sp). Dialyneury formed between pallial nerve of left pleural ganglion and osphradial nerve of supraesophageal ganglion at junction of mantle roof and floor. Single visceral ganglion present at base of cephalic hemocoel.

Female Reproductive System: Gonad (Figs. 77, 79: te) dorsally overlying digestive gland (Fig. 79: dg) from tip of visceral mass to posterior end of gastric chamber (Fig. 79: sto). Oviduct emerging ventrally from ovary. Renal oviduct (Figs. 84, 85: ovi) forming short recurvent loop behind mantle cavity before entering base of glandular oviduct. Pallial oviduct, with proximal albumen (Figs. 84, 85: ag) and distal capsule glands (Figs. 84, 85: cg). Albumen gland forming rear-facing c-shaped tube at posterior end of pallial oviduct; capsule gland developed along dorsal crest of pallial oviduct. Glandular tissue of capsule and albumen glands with opposing flattened surfaces bounding morphologically dorsal gonoductal groove. Narrow vagina along anterior one third of oviduct opening to sperm gutter (Fig. 84: sg) in median lamina. Gutter leading posteriorly to elongate, broad spermatophore bursa (Fig. 84: spb). Inner wall of median lamina fusing to outer wall, restricting communication between spermatophore bursa and ventral channel to elongate, anterior slit (Fig. 84: double dashed line). Ventral edge of median lamina inner wall (Fig. 84: single dashed line) continuing posteriorly as shallow groove above ventral channel, posteriorly enclosing entrance to seminal receptacle (Figs. 84, 85: rcs). Communication between sperm gutter and ventral channel bounded by two folds: one prominent dorsal fold along outer ventral edge of median lamina inner wall, and one prominent ventral fold extending along ventral edge of vagina. Dorsal and ventral fold fusing posteriorly and rapidly becoming obsolete.

Male Reproductive System: Narrow vas deferens (Fig. 86: vd) emerging ventrally from testes (Figs. 77, 79: te), entering posterior end of prostate at base of mantle cavity. Short distal portion of vas deferens thickened and forming straight seminal vesicle. Prostate glandular, forming flattened tube, opening to mantle cavity through narrow, ventral slit along anterior one third (arrows). Posterior half of prostate separated from anterior half by slight dorsal constriction. Glands of posterior lateral lamina deeply longitudinally grooved; anterior portion of lateral lamina with deep, oblique, rear-facing ledge extending ventrally from dorsal constriction to above aperture. Deep grooves from posterior lateral lamina continuous under ledge, toward aperture of spermatophore forming organ. Posterior medial lamina more weakly longitudinally grooved; anterior medial lamina rather smooth. Dorsal, anterior portion of prostate forming elongate, glandular, tube-like spermatophore-forming organ (Fig. 86: sfo). Organ terminating blindly anteriorly, communicating posteriorly with gonoductal groove via narrow aperture.

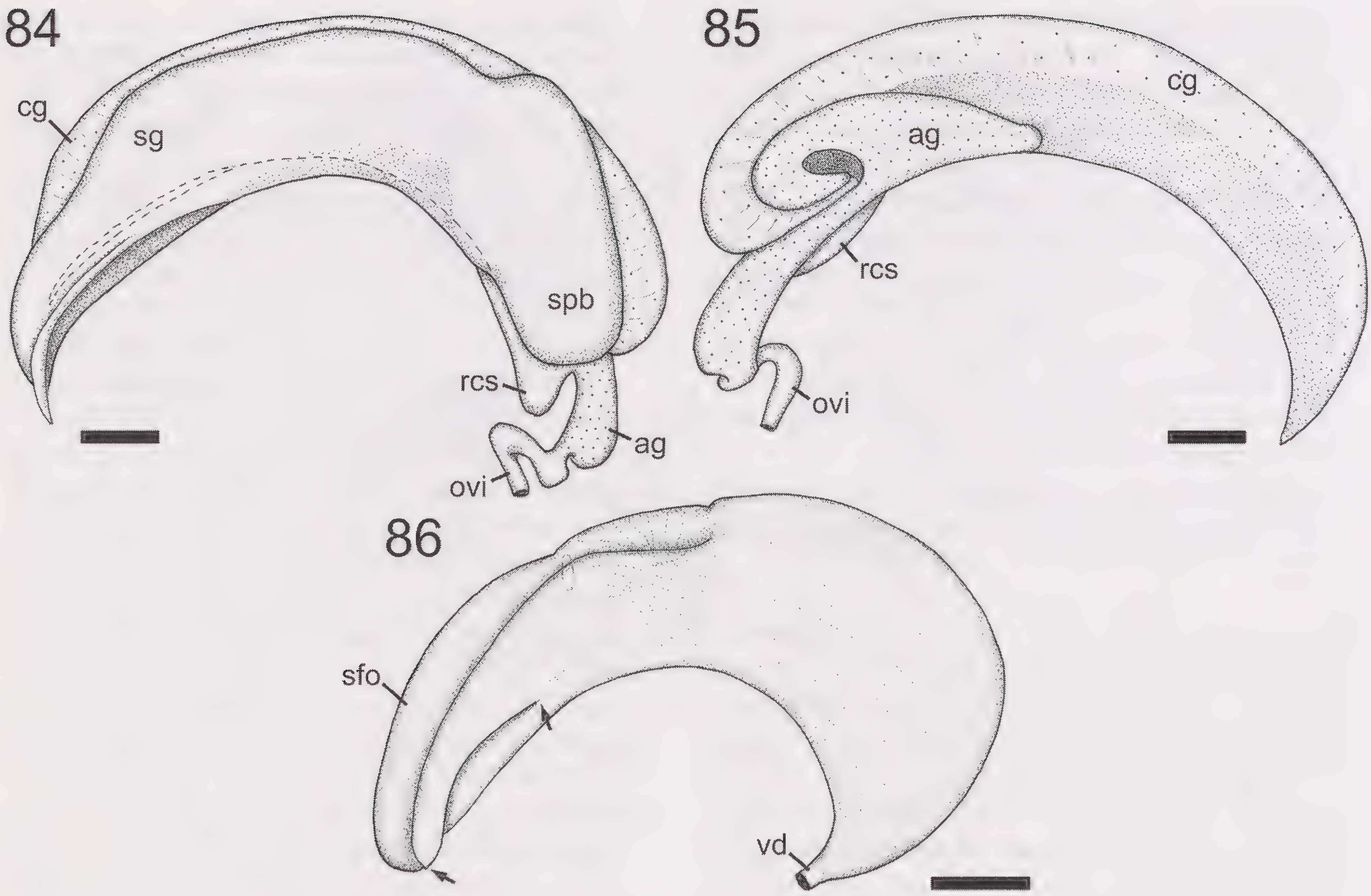

FIGS. 84–86. Reproductive anatomy of *Paramelania iridescens* (ZMB 220.099, except when noted). FIG. 84: External, left lateral view of pallial oviduct. Anterior is at left; FIG. 85: External, right lateral view of pallial oviduct. Anterior is at right; FIG. 86: External, left lateral view of prostate (ZMB 220.037). Anterior is at left. Arrows indicate extent of opening to gonoductal groove. Prominent grooves of lateral lamina seen by transparency. Abbreviations: ag, albumen gland; cg, capsule gland; ovi, renal oviduct; rcs, seminal receptacle; sfo, spermatophore forming organ; sg, seminal groove; spb, spermatophore bursa; vd, vas deferens. Scale bars = 1 mm.

Remarks: Moore (1899b) described the anatomy of *Paramelania iridescens* (as *Bythoceras iridescens*) and correctly pointed out the very different anatomical features as compared to *Lavigeria* (as *Nassopsis*) despite similarity in shell form. Among the features described by Moore (1899b) include the short radular sac and small buccal mass, the presence of a crystalline style and two digestive gland ducts. He stated the salivary glands were similar to those of *Tiphobia*, which he incorrectly described as long and branched (Moore, 1898). He correctly likened the nervous system to that of *Tanganycia* (among others), characterized in particular by dialyneury on the right. He compared the radular dentition to the Melanio-planaxoid type (Moore, 1899a) in determining the affinities to be cerithioid (near *Cerithium* and *Tympanotonus*). Although not stated explicitly in the text, the figure appears to show a rachidian with ~5/1/~5; lateral teeth with 2/1/~6; similar marginal teeth with ~7/~9. The spermatophore forming organ was considered to be lacking by Moore (1899b), who had described the structure as a penis in *Tiphobia* (Moore, 1898) (see also Strong & Glaubrecht, 2002).

Leloup (1953) also provided some information on the operculum and radula with a rachidian broader than tall with 5–6/1/5–6; lateral teeth with 2/1/8–9; similar marginal teeth, each with 6–9 denticles. West & Cohen (1996) reported three layers of crossed lamellar microstructure in the shell. As discussed by Glaubrecht (2008), Brown (1994) reported that females of the genus may be ovoviviparous based on the enlarged lower oviduct figured by Moore (1899b). Despite conchological similarities to the ovoviviparous *Lavigeria*, there is no evidence to suggest that this is true; the present anatomical investigations confirm an oviparous reproductive mode at least for *P. iridescens*. Glaubrecht (2008) provided information on the shell, operculum, radula, external anatomy and ecology (as *P. crassigranulata*). Glaubrecht (2008) indicated that the radula is similar to that of *Paludomus* and *Cleopatra*, but these latter two taxa possess rachidian and lateral teeth that are not so finely and sharply cusped (the prominent central cusp may be squarish, the denticles are more bluntly rounded and may be more similar in size), and marginals with broad, rounded ends and blunt denticles distributed only at the tips.

DISCUSSION

The overriding impression left by this investigation is of remarkable anatomical similarity despite significant differences in shell morphology (Table 1). Anatomical features among the taxa studied here are broadly similar, with organ systems built upon essentially the same plan; this is particularly evident in comparing anatomy of the radula, midgut, kidney and reproductive systems. *Tiphobia* shares this similarity in organization (Strong & Glaubrecht, 2007), as does *Paramelania*, while being a conchological outlier among this assemblage. Several noteworthy differences in the operculum (concentric), midgut (accessory pad) and nervous system (dialyneurous on the right) of *Paramelania* are also present in *Tanganyicia* and *Tiphobia*. But these likely represent plesiomorphic conditions as they occur in *Paludomus* – a fluviatile member of the Paludomidae distributed in Asia.

As stated above, one of the goals of this study is to explore the anatomical data in light of the results of molecular investigations (West & Michel, 2000; Michel, 2004; Wilson et al., 2004). The main difficulty in attempting to assess affinities of tiphobiines based on anatomical characters is that there are apparently few sources of meaningful variation. For example, many of the anatomical differences evident among the tiphobiines represent autapomorphic modifications that do not provide grouping information (e.g., mantle papillae, egg groove, sac-like spermatophore), are difficult to quantify (shape characters relating to, for example, shape of sorting area, glandular pad, pallial gonoduct), or are highly variable and of limited value in assessing affinities (e.g., tooth denticle number). Some variable features almost certainly reflect differences in size. For example, size of the intestinal loop overlying the style sac seems to be strongly correlated with decreasing animal size among syrnolopsines (Strong & Glaubrecht, 2008). Consequently, the presence or absence of the proximal intestinal loop cannot be considered independent evidence of relationship. Other sources of variation likely reflect differences in sexual maturity, at least in part. For example, size of the seminal receptacle and size and shape of the bursa vary to some extent depending on seasonal variations and sexual maturity. Other superficially variable characters likely reflect preservational artifacts. This is certainly true of some of the fine folding patterns within the midgut (u-shaped fold, caecal folds, accessory marginal fold), which can be expected to be sensitive to distortion caused by midgut contents and/or poor preservation.

Despite this caveat, this investigation has revealed several instances of special similarity that may indicate a close relationship between some taxa. For example, *Chytra* and *Limnotrochus* have long been considered to be allied (Digby, 1902; Pilsbry & Bequaert, 1927), but united by features that are not necessarily unique, such as the operculum, radula and oviparous reproductive mode. The present analysis has revealed that *Chytra* and *Limnotrochus* also share features of the salivary glands (branching) and spermatophore bursa (long, broad; elongate fold above ventral channel absent). Aspects of the ovipositor pore (u-shaped lumen), esophagus (dorsal and ventral folding patterns) and spermatophore bursa (elongate fold above ventral channel present) are shared only by *Bathanalia* and *Mysorelloides* within this assemblage, but are not necessarily unique among lake taxa (e.g., ovipositor with a u-shaped lumen – *Syrnolopsis lacustris*; esophageal folding patterns – *Potadomoides*; fold in spermatophore bursa – *Cleopatra*).

Tiphobia possesses a complex mixture of features that are shared with various subsets of tiphobiine taxa, including tubular salivary glands (*Bathanalia*, *Mysorelloides*, *Paramelania*), continuous dorsal and ventral folds in the midesophagus (*Chytra*, *Limnotrochus*, *Paramelania*), and a short, narrow spermatophore bursa (*Chytra*, *Limnotrochus*). No unique anatomical features were found that support the suggested affinity between *Tiphobia* and *Bathanalia* based on their spiny shells and misconception of an ovoviviparous reproductive mode in the latter (see Remarks, Table 1).

In addition, unlike several well characterized subsets of paludomids [e.g., *Lavigeria* plus *Potadomides* (Glaubrecht & Strong, 2007); Syrnolopsini (Strong & Glaubrecht, 2008)], no unique character was found that is shared by all tiphobiines. The aforementioned similarities in

TABLE 1. Summary of major morphological differences. As in the text, formula for radular tooth descriptions is as follows: (1) rachidian: number of denticles on left side/median cusp/number of denticles on right side, (2) lateral teeth: inner denticles/pronounced cusp/outer denticles, (3) marginal teeth: number of denticles on inner marginal tooth/number of denticles on outer marginal tooth. Spermatophore data from Glaubrecht & Strong (2004); data for *Tiphobia horei* from Strong & Glaubrecht (2007). * – umbilicus present in juveniles of *T. horei*; NA – inapplicable features of the ovipositor in ovoviviparous *T. horei*. Abbreviations: ct, ctenidium; nr, circumesophageal nerve ring; ss, style sac; vc, ventral channel.

	Bathanalia straeleni	*Chytra kirkii*	*Limnotrochus thomsoni*	*Mysorelloides multisulcata*	*Paramelania iridescens*	*Tiphobia horei*
Shell						
Umbilicus	Present	Present	Present	Present	Absent	Absent*
Layers crossed lamellar structure	2	3	4	3	4	2
Prominent keel	Present	Present	Present	Absent	Absent	Present
External Anatomy						
Operculum (whorls)	Spiral (6)	Spiral (5.5)	Paucispiral (4.5)	Spiral (5)	Concentric, spiral nucleus	Concentric, spiral nucleus
Ovipositor pore	U-shaped	Simple	Simple	U-shaped	?	NA
Egg groove from pore to foot sole	Present	Absent	Absent	Absent	Absent	NA
Hypobranchial gland	Thick	Thin	Thin	Thin	Moderate	Thin
Mantle edge	Papillate	Smooth	Smooth	Smooth	Smooth	Smooth
Osphradium length	~One third ct	~One fourth ct	~One third ct	~Two thirds ct	~One half ct	~One third ct
Alimentary System						
Rachidian	Rectangular/elongate	Squarish	Rectangular/elongate	Rectangular/elongate	Rectangular/broad	Rectangular/elongate
Rachdian denticles	?	6–8/1/6–8	9–13/1/9–13	6–14/1/6–14	2–7/1/2–7	8–15/1/8–15
Lateral denticles	?	5–7/1/9–14	6–7/1/16–20	5–7/1/17–23	2–4/1/10–12	3–6/1/5–16
Marginal denticles	?	~5/~7	~28–32/~28–32	~20–25/~30–35	~13–16/~13–16	5–8/1–3
Outer edge of outer marginal	?	Smooth	Smooth	Cuspate	Smooth	Smooth

(continues)

(continued)

	Bathanalia straeleni	*Chytra kirkii*	*Limnotrochus thomsoni*	*Mysorelloides multisulcata*	*Paramelania iridescens*	*Tiphobia horei*
Dorsal/ventral folds in midesophagus	Fusing	Continuous	Continuous	Fusing	Continuous	Continuous
Salivary glands	Tubular	Branching	Branching	Tubular	Tubular	Tubular
Salivary gland position	Through nr	Through nr	Through nr	Through/by-pass nr	Through nr	Through nr
Accessory pad	Absent	Absent	Absent	Absent	Present	Present
Caecal folds	1	1–2	1	1	1	1
Caecum	Present	Present	Present	Absent	Present	Present
U-shaped fold	Present	Absent	Present	Present/Absent	Present	Present
Proximal intestine loop overlying ss	Absent	1 large	1 large	1 small	1 large	2 large
Nervous System						
Cerebral nerves	6	6	6	6	6–7	7
Accessory pedal nerves	5	7–8	6	5–7	4–5	6
Subesophageal nerves	3	5	4	5	2	2
Dialyneury/ zygoneury	Zygoneury	Zygoneury	Zygoneury	Zygoneury	Dialyneury	Dialyneury
Supraesophageal connective	Long	Very long	Long	Long	Long	Long
Reproductive System						
Spermatophore bursa	Long, broad	Short, narrow	Short, narrow	Long, broad	Long, broad	Short, narrow
Connection between bursa and vc	Long	Medium, anterior	Short, anterior	Short, anterior	Medium, anterior	Short, anterior
Prominent fold in bursa above connection to vc	Present, continuous posteriorly	Absent	Absent	Present, continuous posteriorly	Present anteriorly above connection to vc only	?
Spermatophore organ	?	Short	?	Short	Elongate	Elongate
Spermatophore	?	Bifurcate, spines	Simple sac	Bifurcate, spines	Bifurcate	Bifurcate

midgut, gonoduct and kidney organization are also present in *Tanganyicia* (Strong & Glaubrecht, 2002) and may be plesiomorphic among Lake Tanganyika paludomids. The significance of these similarities and differences is not yet clear and several possibilities seem most likely: (1) this assemblage may comprise a paraphyletic grade, (2) in the context of a global phylogeny including all taxa, and all available morphological and molecular evidence, monophyly of the Tiphobiini may nevertheless obtain, supported by at least some of the similarities in organization, (3) this grade or clade also includes *Tanganyicia*, although molecular data have consistently placed it apart. These hypotheses remain to be tested.

ACKNOWLEDGEMENTS

We thank the following for their invaluable assistance with specimens under their care: Ian Loch (AMS), Kathie Way (BMNH), Thomas Kristensen (DBL), Jackie van Goethem (IRSNB), and Virginie Héros (MNHN). We are grateful to Heinz H. Büscher (Basel) and Anthony Wilson (Zurich) who collected some of the alcohol preserved material used in this study. We are indebted to Marilyn Schotte (USNM) for inking the anatomical drawings. This study was funded in part by a grant of the Deutsche Forschungsgemeinschaft to MG (GL 297/5-1).

LITERATURE CITED

ANCEY, C.-F., 1882, Les coquilles du lac Tanganyika. *Le Naturaliste*, 4: 38–39.

BANDEL, K., 1998, Evolutionary history of East African fresh water gastropods interpreted from the fauna of Lake Tanganyika and Lake Malawi. *Zentralblatt für Geologie und Paläontologie*, (1)1/2: 233–292.

BOUCHET, P. & J.-P. ROCROI, 2005, Classification and nomenclator of gastropod families. *Malacologia*, 47: 1–397.

BOUILLON, J., 1955, Sur l'anatomie et la position systématique du gasteropode thalassoide *Martelia tanganyicensis* Dautzenberg, 1908. *Revue de Zoologie et Botanique de l'Afrique*, 52: 233–240.

BOURGUIGNAT, J. R., 1886, Des tiphobies du lac Tanganika. *Bulletins de la Société Malacologique de France*, 3: 141–150.

BOURGUIGNAT, J. R., 1888, *Iconographie malacologiques des animaux mollusques fluviatiles du lac Tanganika*. Imprimerie Crété, Corbeil, 82 pp.

BROWN, D. S., 1994, *Freshwater snails of Africa and their medical importance, revised 2nd ed.* Taylor & Francis, London, x + 609 pp.

DIGBY, L., 1902, On the structure and affinities of the Tanganyika gastropods *Chytra* and *Limnotrochus*. *Journal of the Linnean Society London, Zoology*, 28: 434–442.

GLAUBRECHT, M., 1996, *Evolutionsökologie und Systematik am Beispiel von Süß- und Brackwasserschnecken (Mollusca: Caenogastropoda: Cerithioidea): Ontogenese-Strategien, paläontologische Befunde und historische Zoogeographie*. Backhuys, Leiden, xvi + 499 pp.

GLAUBRECHT, M., 1999, Systematics and evolution of viviparity in tropical freshwater gastropods (Cerithioidea: Thiaridae *s.l.*). *Courier Forschungs-Institut Senckenberg*, 203: 91–96.

GLAUBRECHT, M., 2008, Adaptive radiation of thalassoid gastropods in Lake Tanganyika, East Africa: morphology and systematization of a paludomid species flock in an ancient lake. *Zoosystematics and Evolution*, 84: 69–120.

GLAUBRECHT, M. & E. E. STRONG, 2004, Spermatophores of thalassoid gastropods (Paludomidae) in Lake Tanganyika, East Africa, with a survey of their occurrence in Cerithioidea: functional and phylogenetic implications. *Invertebrate Biology*, 123: 218–236.

GLAUBRECHT, M. & E. E. STRONG, 2007, Ancestry to an endemic radiation in Lake Tanganyika? The viviparous gastropod *Potadomoides* Leloup, 1953 in the Congo River system (Caenogastropoda, Cerithioidea, Paludomidae). *Biological Journal of the Linnean Society*, 92: 367–401.

LELOUP, E., 1953, *Exploration hydrobiologique du Lac Tanganika (1946–1947). Volume 3, Fascicule 4, Gastéropodes*. Institut Royal des Sciences Naturelles de Belgique, Bruxelles, 273 pp.

MANDAHL-BARTH, G., 1954, The anatomy and systematic position of the Tanganyika snails *Syrnolopsis* and *Anceya*. *Annales du Musée Royal de l'Afrique Centrale, Sciences Zoologiques, Tervuren, Belgium*, 1: 217–221.

MICHEL, E., 2004, *Vinundu*, a new genus of gastropod (Cerithioidea: 'Thiaridae') with two species from Lake Tanganyika, East Africa, and its molecular phylogenetic relationships. *Journal of Molluscan Studies*, 70: 1–19.

MOORE, J. E. S., 1898, The molluscs of the Great African Lakes. II. The anatomy of the *Typhobias*, with a description of the new genus (*Batanalia*). *Quarterly Journal Microscopic Sciences*, 41: 181–204.

MOORE, J. E. S., 1899a, The molluscs of the Great African Lakes. III. *Tanganyikia rufofilosa*, and the genus *Spekia*. *Quarterly Journal Microscopic Sciences*, 42: 155–185.

MOORE, J. E. S., 1899b, The molluscs of the Great African Lakes. IV. *Nassopsis* and *Bythoceras*. *Quarterly Journal Microscopic Sciences*, (n.s.), 42: 187–201.

MOORE, J. E. S., 1903, *The Tanganyika problem*. Hurst & Blackett, London, xxiii + 371 pp.

PILSBRY, H. A. & J. BEQUAERT, 1927, The aquatic mollusks of the Belgian Congo. With a geographical and ecological account of Congo malacology. *Bulletin American Museum of Natural History*, 53: 69–602.

RIEDEL, F., 1993, Early ontogenetic shell formation in some freshwater gastropods and taxonomic implications of the protoconch. *Limnologica*, 23: 349–368.

SMITH, E. A., 1880, Diagnoses of new shells from Lake Tanganyika and East Africa. *Annals and Magazine of Natural History*, 1880: 425–430.

SMITH, E. A., 1881, On a collection of shells from Lakes Tanganyika and Nyassa and other localities in East Africa. *Proceedings of the Zoological Society of London*, 1881: 276–300.

STRONG, E. E. & M. GLAUBRECHT, 2002, Evidence for convergent evolution of brooding in a unique gastropod from Lake Tanganyika: anatomy and affinity of *Tanganyicia rufofilosa* (Smith, 1880) (Caenogastropoda, Cerithioidea, Paludomidae). *Zoologica Scripta*, 31: 167–184.

STRONG, E. E. & M. GLAUBRECHT, 2003, Anatomy and systematic affinity of *Stanleya neritinoides* (Smith, 1880), an enigmatic member of the thalassoid gastropod fauna from Lake Tanganyika, East Africa (Cerithioidea, Paludomidae). *Acta Zoologica*, 84: 249–265.

STRONG, E. E. & M. GLAUBRECHT, 2007, The morphology and independent origin of ovoviviparity in *Tiphobia* and *Lavigeria* (Caenogastropoda, Cerithioidea, Paludomidae) from Lake Tanganyika. *Organisms, Diversity and Evolution*, 7: 81–105.

STRONG, E. E. & M. GLAUBRECHT, 2008, Anatomy and systematics of the minute syrnolopsine gastropods from Lake Tanganyika (Caenogastropoda, Cerithioidea, Paludomidae). *Acta Zoologica*, 89: 289–310.

THIELE, J., 1929–1935, *Handbuch der systematischen Weichtierkunde*. Fischer, Jena, vi + 1154 pp.

WEST, K. & A. COHEN, 1996, Shell microstructure of gastropods from Lake Tanganyika, Africa: adaptation, convergent evolution and escalation. *Evolution*, 50: 672–682.

WEST, K. & E. MICHEL, 2000, The dynamics of endemic diversification: molecular phylogeny suggests an explosive origin of the thiarid gastropods of Lake Tanganyika. *Advances in Ecological Research*, 31: 331–354.

WILSON, A. B., M. GLAUBRECHT & A. MEYER, 2004, Ancient lakes as evolutionary reservoirs: evidence from the thalassoid gastropods of Lake Tanganyika. *Proceedings of the Royal Society of London, Biological Sciences*, 1538: 529–536.

YONGE, C. M., 1938, The prosobranchs of Lake Tanganyika. *Nature*, 142: 464–466.

Revised ms. accepted 16 November 2009